NEA/NSC/DOC(96)20

NEA NUCLEAR SCIENCE COMMITTEE

PWR BENCHMARK ON UNCONTROLLED RODS WITHDRAWAL AT ZERO POWER

Final Report

Roger FRAIKIN
Tractebel Energy Engineering
Brussels, Belgium

September 1997

Nuclear Energy Agency

ORGANISATION FOR ECONOMIC CO-OPERATION AND DEVELOPMENT

FOREWORD

Nuclear industries and licensing authorities need to be able to rely on the good performance of methods and computer programs used in safety analysis calculations. This is best achieved through validation and benchmarking on an international scale.

Benchmarks in which these codes are compared against sets of data from nuclear power plant operation, from specifically designed "clean" measurements, or from mathematically well defined problems have been organised and successfully concluded under the auspices of the OECD Nuclear Energy Agency on several topics. These benchmark studies aim at verifying the correctness of methods and computer codes, building confidence in areas where experiment is very expensive or lacking.

A task group addressing the subject of Light Water Reactor core transients was set up under the former committee on reactor physics about five years ago. This activity has been taken over by the Nuclear Science Committee. The present report summaries a project carried out in the frame of Nuclear Science Committee activities concerning reactivity accidents in Pressurised Water Reactors.

The benchmark specification was prepared by Roger Fraikin (Tractebel Energy Engineering) and Herbert Finnemann (Siemens KWU) with the assistance of several other participants. Ph. Brohan and P.K. Hutt (Nuclear Electric) calculated the reference solution. The present work was co-ordinated by Roger Fraikin, who also prepared this report.

Apart from the benchmark discussed here, the following other benchmarks have been investigated or are in process of being initiated:

- H. Finnemann, H. Bauer, A. Galati, R. Martinelli, *Results of LWR Core Transients Benchmarks*, NEA/NSC/DOC(93)25, October 1993, comprising:
  - three cases of a rod ejection at Zero Power in a PWR;
  - three cases of a rod ejection at Full Power in a PWR;
  - a cold water injection and core pressurisation transient in a BWR.
- T. Lefvert, *Ringhals 1 Stability Benchmark,* NEA/NSC/DOC(96)22, November 1996.
- T. Lefvert, *BWR Time Series Analysis* – proposed 1996.
- K.N. Ivanov and A.J. Baratta, *Proposal for a Benchmark on Coupled Thermal-Hydraulic Spatial Kinetics Codes for LWR Analysis,* PWR Main Steam Line Break Benchmark – proposed 1996.
- R. Fraikin, *Loss of Flow Accident (LOFA) Transients in a PWR* – to be prepared in 1997.

The opinions expressed in this report are those of the author only and do not necessarily represent the position of any Member country or international organisation. This report is published on the responsibility of the Secretary-General of the OECD.

Acknowledgements

This report is dedicated to the memory of Renato Martinelli, who was the initiator of this series of benchmark activity, and who has personally contributed in an essential way to its success.

The author would like to thank Dr. P.K. Hutt, from Nuclear Electric and Dr. H. Finnemann for their help in preparing the specification of this benchmark.

Without a reference solution, this final report would have lost much of its interest. Philip Brohan (Nuclear Electric) has not spared in his efforts to prepare that solution, nor in investigating any possible issue concerning it, and should be thanked for that. The help of Jim Kuijper, from Energieonderzoek Centrum Nederland, was also appreciated.

This report is the sum of many comments, suggestions and sensitivity analyses performed by the participants.

Co-ordinating this benchmark was a great experience for the author, who is grateful to all the participants for the quality of the contacts that were established during the benchmarking and reporting process, and for their dedicated efforts in this benchmark.

Finally, the author was very pleased to work with Dr. Enrico Sartori, who supported the benchmark by efficiently handling administration, organising the meetings and, last but not least, providing valuable and friendly advice.

TABLE OF CONTENTS

FOREWORD 3

ACKNOWLEDGEMENTS 4

EXECUTIVE SUMMARY 9

1. Introduction 11

2. Conclusions 11

3. Benchmark specification 12

3.1 Core description 12

3.2 Transient evolution 12

3.3 Definition of cases 13

4. Participants and methods 14

5. Reference solution 15

5.1 Steady state initial conditions 15

5.2 Transient evolution 15

5.3 Snapshot at time of maximum power 16

5.4 T&H discussion 16

6. Participants' solutions 17

6.1 Remarks 17

6.2 Steady state initial conditions 17

6.2.1 Critical boron concentration (B1) 17

6.2.2 Axial peak factor Fz (B2) 18

6.2.3 Radial peak factor Fxy (B3) 19

6.2.4 Peak factor in axial layer 6 (B4) 19

6.2.5 Peak factor in axial layer 13 (B5) 20

6.2.6 Global (3-D) peak factor FQ (B6) 20

6.3 Transient evolution (core average) 21

6.3.1 General remarks about the analysed cases 21

6.3.2 Maximum fission power (C1) 22

6.3.3 Time of maximum fission power (C1) 23

6.3.4 Maximum of coolant heating (C2) 23

6.3.5 Maximum of coolant outlet temperature (C3) 24

6.3.6 Maximum of fuel Doppler temperature (C4) 25

6.4 Transient evolution (hot pellet) 25

6.4.1 Introduction 25

6.4.2 Maximum fission power in hot pellet w/r to nominal power (D1) 26

6.4.3 Maximum coolant heating in hot pellet w/r to average nominal power (D2) 27

6.4.4 Maximum coolant temperature at outlet of hot channel (D3) 28

6.4.5 Maximum heat exchange coefficient between cladding and moderator in hot pellet (D4) 28

6.4.6 Minimum heat exchange coefficient between cladding and moderator in hot pellet (D4) 29

6.4.7 Maximum fuel enthalpy in hot pellet (D5) 29

6.4.8 Time of maximum fuel enthalpy in hot pellet (D5) 30

6.4.9 Maximum fuel temperature at centreline of hot pellet (D6) 30

6.4.10 Maximum hot pellet cladding outer surface temperature (D7) 31

6.5 Snapshot at time of maximum power 31

6.5.1 Maximum fission power (E1) 32

6.5.2 Axial peak factor Fz (E2) 32

6.5.3 Radial peak factor Fxy (E3) 33

6.5.4 Radial peak in axial layer 6 (E4) 33

6.5.5 Radial peak in axial layer 13 (E5) 34

6.5.6 Global (3-D) peak factor FQ (E6) 34

REFERENCES 35

APPENDIX A – List of participants and contributors 37

APPENDIX B – Time histories plots 39

APPENDIX C – Axial power profiles 59

APPENDIX D – Radial power profiles 67

List of tables

Table 1. List of participants 14

Table 2. Models 14

Table 3. Reference solution – initial steady state conditions 15

Table 4. Transient core averaged results – reference 15

Table 5. Transient hot pellet results – reference 16

Table 6. Snapshot at time of maximum fission power – reference 16

Table 7. Intra-assembly T&H channels discretisation influence 16

Table 8. Initial critical boron concentration (ppm) 18

Table 9. Inital axial peak factor (Fz) 18

Table 10. Initial radial peak factor (Fxy) 19

Table 11. Initial peak factor in axial layer 6 19

Table 12. Initial peak factor in axial layer 13 20

Table 13. Initial global (3-D) peak factor 20

Table 14. Consistency check on initial FQ, based on items B6 and D1 21

Table 15. Maximum fission power (C1) 22

Table 16. Time(s) of maximum fission power (C1) 23

Table 17. Maximum of the coolant heating (C2)..... 24

Table 18. Maximum coolant outlet temperature (C3), in °C..... 24

Table 19. Maximum fuel Doppler temperature (C4), in °C..... 25

Table 20. Maximum fission power in hot pellet w/r to nominal power (D1)..... 27

Table 21. Maximum coolant heating in hot pellet w/r to average nominal power (D2)..... 27

Table 22. Maximum coolant temperature at outlet of hot channel (D3), in °C..... 28

Table 23. Maximum cladding/moderator heat exchange coefficient in hot pellet (D4)..... 28

Table 24. Minimum cladding/moderator heat exchange coefficient in hot pellet (D4)..... 29

Table 25. Maximum fuel enthalpy injected in hot pellet (D5)..... 30

Table 26. Time(s) of maximum fuel enthalpy in hot pellet (D5)..... 30

Table 27. Maximum fuel temperature at centreline in hot pellet (D6), in °C..... 31

Table 28. Maximum hot pellet cladding outer surface temperature (D7), in °C..... 31

Table 29. Axial peak factor Fz at time of maximum fission power (E2)..... 32

Table 30. Radial peak factor Fxy at time of maximum fission power (E3)..... 33

Table 31. Radial peak in axial layer 6 at time of maximum fission power (E4)..... 33

Table 32. Radial peak in axial layer 13 at time of maximum fission power (E5)..... 34

Table 33. Global (3-D) peak factor FQ at time of maximum fission power (E6)..... 34

EXECUTIVE SUMMARY

The evolution of safety analysis methods parallels the advances in fuel management and computer technology [18]. Limited by computational power, earlier safety methods used a simple point kinetics core response in conjunction with a conservative approach for physics input in order to bound fuel operation. With the implementation of advanced fuel management, margins to safety and licensing limits were frequently reduced. This led to general development of advanced methods that reduce the level of conservatism by implementing kinetics methods that more accurately capture spatial effects occurring during reactor transients.

The performance of numerical methods needs to be established over a realistic range of applications. NEA-NSC has organised several benchmarks aiming to evaluate the accuracy of 3-D and 1-D space-time kinetics codes in transient calculations. A former benchmark analysed the "rod ejection" accident [1,3]. This paper presents the results of the "rod withdrawal from zero power" benchmark, including the solutions obtained by ten participants, from ten different countries, and a reference solution, obtained by refining the spatial and time meshing.

The problem is mathematically well defined. The specification [4] provides cross-sections for fuel, reflector and absorbers. Four cases are analysed. The submitted solutions are compared to a reference obtained with a nodal code using finer spatial and temporal resolution than in standard calculation. Besides global information such as fission power evolution, the set of results also includes local maxima, as well as hot pellet enthalpy and cladding temperature.

In general, a good agreement is obtained for most of the codes on the power evolution and its integral, in particular for the core averaged parameters. For the "hot pellet", the spread of the results is more important; however, the assumptions that define and localise this pellet are not the same for each participant: a finer local power profile reconstruction leads to more severe effects. This shows that one must take care of the consistency between the calculation methodology and the criteria applied to the safety analyses.

Only one code uses a 1-D model. It is interesting to see that its results do not differ much from those obtained from 3-D models, except for the expected overestimation due to the 2D*1D factorisation method. This light over-conservatism could often be accepted for safety analyses.

The large interest expressed by non participants to this benchmark [18,20] and to the preceeding one shows that a real need exists for such exercises because of the lack of measurements on reactivity insertion transients. Projects of future work have been proposed. A benchmark on the main steam line break is in preparation. The analysis needs a coupling between spatial kinetics and thermal-hydraulics codes. A benchmark on the LOFA (loss of flow accident) will also be launched [15,16].

1. Introduction

There has been a great interest in the rod ejection NEA-NSC benchmark launched [1] in 1991 and reported [3,5] by H. Finnemann in 1993. Many companies have used the data to validate their own codes after the presentation of the final report.

A second benchmark was therefore submitted [2] for the approval of NEA-NSC. The idea was to use the same core model as in the former benchmark, to validate the codes for another of the standard problems of PWR core safety analysis: the rod withdrawal at zero power accident.

The transient consists in the withdrawal of one or several banks, starting at criticality with a very low power level (10^{-13} times nominal value).

In September 1993, NEA published the final specifications [4], prepared by Tractebel and Siemens AG/KWU. Four cases are defined:

- Cases A, B and D differ by the localisation of the involved rod banks and in consequence the injected reactivity.

- Case C is the same as Case B, except that the fuel-water heat transfer coefficient is fixed. The possible influence of the choice of a correlation for the T&H (Thermal & Hydraulics) had indeed been questioned for the former benchmark.

With respect to the rod ejection benchmark, the set of results was enhanced by adding safety related output, as well as hot pellet enthalpy, cladding temperature, etc.

Tractebel agreed to co-ordinate the benchmark.

An intermediate meeting [16] was held in May 1995, in Paris. The participants could share their experiences [7-14] and were allowed to correct their data. The rod ejection benchmark had indeed shown the interest to detect and solve any possible specification misunderstanding.

A summary report [21] was presented in September 1996, at the PHYSOR'96 meeting held in Mito, Japan.

Finally, ten participants agreed to have their results published in the present report.

2. Conclusions

A good agreement is obtained for most of the codes on the power evolution and its integral.

However, the power surge does not occur simultaneously for all participants: it starts a few seconds earlier than average for the 1-D code OKAPI, and a few seconds later for Cesar, Coccinelle, Quandry-En and Arotta-3D. In Case D, the two Panther's solutions differ by about one second.

In general, a good agreement is obtained for most of the codes on the power evolution and its integral, in particular for the core averaged parameters. For the "hot pellet", the spread of the results is more important; however, the assumptions that define and localise this pellet are not the same for

each participant: a finer local power profile reconstruction leads to more severe effects. This shows that one must take care of the consistency between the calculation methodology and the criteria applied to the safety analyses.

The axial and radial power distributions are very similar for all of the participants as far as the whole core is concerned. The axial envelope profiles reflect the differences obtained at the "hot pellet" level.

Only one code uses a 1-D model. It is interesting to see that its results do not differ much from those obtained from 3-D models, except for the expected overestimation due to the 2D*1D factorisation method. This light over-conservatism could often be accepted for safety analyses.

The large interest expressed by non-participants to this benchmark [18,20] and to the former one (rod ejection) shows that a real need is found for such exercises, because of the lack of measurements on reactivity insertion transients.

Projects for future work have been proposed. OECD recently distributed a "draft" specification of a benchmark on the main steam line break. This analysis requires a coupling between spatial kinetics and thermal-hydraulics codes. It was also decided to launch a benchmark on the LOFA (loss of flow accident) [15,16].

3. Benchmark specification

3.1 Core description

This benchmark is based on the same core model as the NEACRP PWR 3-D core transient benchmark (rod ejection accident) described in [1]. This model is directly derived from real reactor geometry and operation data.

The load (157 assemblies) corresponds to a "first cycle". This eliminates the need to model Samarium and burn-up axial distribution and simplifies the data tables. However, it increases the number of tables: eleven compositions are defined, with different ^{235}U enrichments and number of burnable absorber rods.

The specification [4], details the core geometry, the neutron modelling (two prompt neutron groups, i.e. thermal and fast neutrons, and six delayed neutron groups), and boundary conditions. It provides a complete set of macroscopic cross-sections for transport, scattering, absorption and fission and their derivatives with respect to boron density, moderator temperature, moderator density, and fuel temperature. The latter is a combination of centreline and surface temperature in UO_2. Thermophysical properties of fuel and cladding are given as polynomial correlation.

The specification corresponds finally to a mathematically well defined problem.

3.2 Transient evolution

From a critical initial state at zero power (10^{-13} time nominal power), one or two control rod banks are withdrawn, at maximum speed (72 steps/minute). The evolution consists basically in a continuous

reactivity insertion, limited by the reactor trip, that occurs a certain delay (0.6 s) after high flux detection (35% nominal fission power).

Because of this delay, the main factor limiting the consequences of the accident remains the Doppler effect, as in the rod ejection benchmark. The temperature rise and the reactivity insertion, however, are stopped by the trip, that must therefore be taken into account.

With a high reactivity insertion rate, as usually taken into account for safety analyses, the transient produces a fast power burst. In this case, the maximum power is less important than its time integral, i.e. the amount of energy injected to the fuel pellet.

If the reactivity insertion rate is low, the heating of the fuel may be sufficient to have Doppler anti-reactivity balancing the inserted reactivity while the power level is still under the trip level. This was observed for Case A, as explained hereafter.

3.3 Definition of cases

Four cases are defined:

- Case A represents a single bank (D) withdrawal, other banks (C,B,A,S) remaining fully withdrawn until scram; bank D weights about 1400 pcm;

- Case B represents a double bank (B+C) withdrawal; at initial conditions, control banks (D,C,B,A) are fully inserted, while shutdown banks (S) remain fully withdrawn until scram; banks B+C weight about 3800 pcm of reactivity;

- Case C is almost identical to Case B, except that the heat transfer coefficient between cladding and water is set constant to 30 000 W/m2/C;

- Case D starts from the same initial conditions as Case B, but withdraws the more peripheral rods (A+B), inserting about 3200 pcm of reactivity.

Remarks about these cases:

- Cases B, C, D are close to those usually considered for safety analysis. The control banks are initially inserted, and two groups are withdrawn. The power surge is far above the trip level. It is stopped by the Doppler feedback; the shutdown then stops the reactivity insertion and limits the fuel heating.

- Case C is identical to Case B, except that the heat transfer coefficient between fuel and moderator is specified as a constant value. The aim is to evaluate the influence of the choice of the heat transfer correlation. This point had indeed been questioned for the former benchmark. Actually, a very little effect is observed. The reason is that the water temperature remains low, even in the "hot" channel.

- In Case A, only one rod bank is withdrawn, while all the other banks remain fully extracted until SCRAM. This case provides interesting results: because of the lower rod worth, the power increase is slower. A sufficient fuel heating is obtained, just below 35% power, to balance the reactivity insertion with the Doppler feedback. The power excursion is thus stopped, and a first power peak is observed. However, the rod extraction forces the power

to continue a slow increase, so that the shutdown is triggered about 10 s later. In this way, a significant amount of power is maintained long enough to produce a higher enthalpy build-up than in the other cases, although the reactivity insertion rate is lower.

4. Participants and methods

Table 1 shows that not all participants did calculate the full set of cases. However, a full comparison is possible for Case B (all participants), and Case A (except for Framatome). In addition, a few codes were not able to output the full set of specified results, which explains why some cells are empty, and some curves do not appear in the appendices.

Table 1. List of participants

Country	Participant	Code	Results for Case			
			A	B	C	D
B	Tractebel	Okapi	x	x	x	x
D-HR	GRS & Univ. Zagreb	Quabox-Cubbox-Hyca	x	x	x	x
D	KWU	Panbox	x	x	x	x
F	EDF	Coccinelle	x	x		
F	Framatome	Cesar		x		
GB	Nucl. Electric	Panther	x	x	x	x
I	ENEL	Quandry-En	x	x		
NL	ECN	Panther	x	x	x	x
RC	INER	Arotta-3D	x	x	x	x
USA	Studsvik	Simulate	x	x	x	x

Table 2 compares the space models and discretisations used, showing that most of the codes use a nodal model, except for Cesar and OKAPI, which use a fine spatial mesh. The method used to calculate the power in the "hot pellet" and the "hot channel" is abbreviated as follows:

- A: assembly average power
- N: nodal power
- L: local power reconstruction

Table 2. Models

Country	Participant	Code	Spatial discretisation of the core				Hot
			Type	Dim	Axial	Radial	Pellet
		Reference	nodal	3-D	48	3×3	A
B	Tractebel	Okapi	fine	1-D	50	2×2*	L
D-HR	GRS/U.Zagreb	Quab./Cub./Hyca	nodal	3-D	16	1×1	A
D	KWU	Panbox	nodal	3-D	16	1×1	N
F	EDF	Coccinelle	nodal	3-D	30	4×4	N
F	Framatome	Cesar	fine	3-D	38	4×4	N
GB	Nucl. Electric	Panther	nodal	3-D	32	2×2	A
I	ENEL	Quandry-En	nodal	3-D	16	1×1	A
NL	ECN	Panther	nodal	3-D	16	1×1	A
RC	INER	Arotta-3D	nodal	3-D	16	2×2	A
USA	Studsvik	Simulate	nodal	3-D	24	2×2	N

* All the codes are 3-D, except for the Belgian 1-D code "OKAPI" [19]. However, this last provides a full set of results, including 3-D maps. These were obtained by using an axial*radial synthesis, combining axial transient profiles with pre-calculated radial profiles ("adiabatic model"); in the table, "2×2*" refers to this 2-D pre-calculation.

5. Reference solution

During the specialists meeting [16] held at the end of the first iteration, it was decided to calculate a reference solution. Nuclear Electric accepted to perform the calculation, using Panther with a finer spatial and temporal resolution than in standard calculations.

Table 2 shows that the space meshing was refined to 3×3 nodes per assembly, and 48 axial nodes, while the time step was reduced down to the convergence of the results.

This solution was not known to the participants at the time they submitted their final results.

A late result from ECN [17], not shown here, was also calculated using a radial and finer axial mesh; it confirms the results of the reference solution obtained by Nuclear Electric.

5.1 Steady state initial conditions

Table 3 shows the main results. It should be noted that Cases B, C and D are identically defined, as far as initial conditions are concerned. Appendices C and D detail the axial and radial power profiles, comparing the solutions obtained by the participants to the reference.

Table 3. Reference solution – initial steady state conditions

Item	Result	A	B	C	D
B1	Critical boron concentration (ppm)	1262.7	793.6	=B	=B
B2	Axial peak factor (Fz)	1.513	1.507	=B	=B
B3	Radial peak factor (Fxy)	1.242	1.912	=B	=B
B4	Peak factor in axial layer 6	1.542	2.377	=B	=B
B5	Peak factor in axial layer 13	0.811	1.245	=B	=B
B6	Global (3-D) peak factor (FQ)	1.880	2.886	=B	=B

5.2 Transient evolution

Table 4 summarises the global results, while Table 5 gives the envelope results (hot pellet). Appendix B details the evolution, comparing the solutions obtained by the participants to the reference.

Table 4. Transient core averaged results – reference

Item	Result	A	B	C	D
C1	Maximum fission power (%)	35.6	134.8	134.2	96.9
	Time of maximum fission power (s)	82.14	34.30	34.30	39.40
C2	Maximum power to coolant (%)	29.5	13.8	13.7	12.5
C3	Maximum coolant outlet temperature (°C)	295.3	290.5	290.4	290.0
C4	Maximum fuel Doppler temperature (°C)	358.7	315.2	315.4	312.6

Table 5. Transient hot pellet results – reference

Item	Result (maximum of)	A	B	C	D
D1	Fission power (%)	87.7	600.2	598.3	394.3
D2	Coolant heating (%)	75.7	68.2	67.9	57.6
D3	Coolant temper. at outlet (°C)	302.0	297.2	297.1	296.0
D4	T&H heat exch. coeff. ($W/m^2/°C$)	33407	33335	30000	33253
D5	Fuel enthalpy (J/Kg)	187530	171750	171989	164119
D6	Fuel centreline temper. (°C)	631.8	478.2	479.0	451.4
D7	Cladding outer surf. temper. (°C)	308.2	303.6	304.7	301.3

5.3 Snapshot at time of maximum power

Table 6 gives the power peak factors (axial, radial, 3-D) at the time of the maximum power. Appendices C and D detail the axial and radial power profiles, comparing the solutions obtained by the participants to the reference.

Table 6. Snapshot at time of maximum fission power – reference

Item	Result	A	B	C	D
E1	Maximum fission power (%)	35.56	134.80	134.23	96.85
E2	Axial peak factor (Fz)	1.985	2.437	2.435	2.325
E3	Radial peak factor (Fxy)	1.195	1.751	1.751	1.715
E4	Radial peak in axial layer 6	2.395	3.053	3.051	3.120
E5	Radial peak in axial layer 13	0.272	0.322	0.323	0.330
E6	Global (3-D) peak factor (FQ)	2.395	3.967	3.964	3.718

5.4 T&H discussion

The reference solution, as presented here, uses one T&H channel per node (3×3 channels per fuel assembly), while the specification [4] says "one T&H channel per fuel assembly". This issue has been solved by performing supplemental calculations. Table 7 shows that this effect is very limited. It was therefore decided to keep the former results as reference. The maximum coolant temperature at hot channel outlet (D3) is almost independent of the mesh size, as it is assembly averaged in both cases.

Table 7. Intra-assembly T&H channels discretisation influence

Effect of grouping 3´3 nodes in one T&H channel	Case A	Case B	Case C	Case D
Peak power	0	+3.6%	+3.6%	+3.6%
Peak core average fuel temperature	-0.6ºC	+0.7ºC	+0.7ºC	+0.7ºC
Peak fuel centreline temperature	-2.2ºC	+4.8ºC	+4.8ºC	+5.5ºC
Time of power maximum	-0.6 s	0	0	0

The reference solution was initially calculated using a table of water properties slightly different from the standard one. Nuclear Electric repeated the calculation with the most accurate tables with no noticeable differences except the initial critical boron concentration. In § 6.2.1, Table 8 is updated

according to that new “B1” solution, which is therefore slightly different from that presented in Mito [21]. The latter is given in italic in the same table.

6. Participants' solutions

6.1 Remarks

The following tables give for each item the position of the participants with respect to reference solution:

- Each result item is identified here by a symbol (e.g. "E4"), as in the specification [4].

- Average bias and standard deviation give an image of the dispersion of the results. In some cases we had to exclude some "non conforming" results from the statistics. These values are shown in italic.

- The differences, bias and standard deviation, are expressed in per cent of the reference, whenever possible. To avoid any confusion, the reference is never given in per cent, even for power fractions, so that "%" means always "% of the reference result".

6.2 Steady state initial conditions

Because all neutronic data are explicitly given in the specifications, and initial conditions are "clean" (Zero Power, Beginning of Cycle, without Xe, Sm, with flat distribution of burn-up and without feedback), discrepancies should only result from:

- inaccuracy in solving the steady state diffusion problem;

- miscoding the data;

- misunderstanding the specifications.

Misunderstanding and miscoding occurred indeed in some cases, and the problems were discussed in Paris [7,16]. After correction, the consistency became good for most participants, as shown in following tables. This "milestone" was important, because a discrepancy at this stage would of course influence the transient analysis.

The following results have been compared: critical boron concentration, average axial and radial power distributions, axial, radial and 3-D shape factors (Fxy, Fz and FQ), envelope axial power distribution, and "slices" of radial power distribution.

6.2.1 Critical boron concentration (B1)

Table 8 shows that the standard deviation is about 5 to 6 ppm.

Two values are given here for the reference solution and for the bias; the difference lays in the steam tables, thus in the moderator density (see § 5.4 above).

Table 8. Initial critical boron concentration (ppm)

Country	Participant	Code	A	B	C	D
		Reference	**1262.7 (*1268.0*)**	**793.6 *(799.2)***	**793.6 *(799.2)***	**793.6 *(799.2)***
B	Tractebel	Okapi	+1.0	-0.8	-0.8	-0.8
D-HR	GRS/U. Zagreb	Quab./Cub./Hyca	+18.3	+10.3	+10.3	+10.3
D	KWU	Panbox	+4.4	+2.5	+2.5	+2.5
F	EDF	Coccinelle	+3.5	+2.4		
F	Framatome	Cesar		+21.4		
GB	Nucl. Electric	Panther	+5.7	+5.8	+5.8	+5.8
I	ENEL	Quandry-En	+10.3	+7.3		
NL	ECN	Panther	+12.1	+9.2	+9.2	+9.2
RC	INER	Arotta-3D	+7.7	+10.0	+10.0	+10.0
USA	Studsvik	Simulate	-1.5	-0.6	-0.6	-0.6
		Average Bias	**+6.8 *(+1.5)***	**+6.8 *(+1.2)***	**+5.2 *(-0.4)***	**+5.2 *(-0.4)***
		Standard Deviation	**6.1**	**6.6**	**4.9**	**4.9**

6.2.2 Axial peak factor Fz (B2)

Table 9 shows that all the solutions are almost identical, with a typical deviation < 0.5%.

Table 9. Initial axial peak factor (Fz)

Country	Participant	Code	A	B	C	D
		Reference	**1.513**	**1.507**	**1.507**	**1.507**
B	Tractebel	Okapi	-0.002	+0.000	+0.000	+0.000
D-HR	GRS/U.Zagreb	Quab./Cub./Hyca	+0.004	+0.004	+0.004	+0.004
D	KWU	Panbox	-0.001	-0.002	-0.002	-0.002
F	EDF	Coccinelle	-0.002	-0.002		
F	Framatome	Cesar		+0.004		
GB	Nucl. Electric	Panther	+0.000	+0.000	+0.000	+0.000
I	ENEL	Quandry-En	+0.001	+0.000		
NL	ECN	Panther	+0.000	+0.000	+0.000	+0.000
RC	INER	Arotta-3D	-0.007	-0.006	-0.006	-0.006
USA	Studsvik	Simulate	+0.007	+0.007	+0.007	+0.007
		Average Bias	**-0.000**	**+0.001**	**+0.001**	**+0.001**
		Standard Deviation	**0.004**	**0.004**	**0.004**	**0.004**

6.2.3 Radial peak factor Fxy (B3)

Table 10 shows that all the solutions are very close together, with deviations < 1%, except for Quabox and Arotta.

Table 10. Initial radial peak factor (Fxy)

Country	Participant	Code	A	B	C	D
		Reference	**1.242**	**1.912**	**1.912**	**1.912**
B	Tractebel	Okapi	-0.004	-0.005	-0.005	-0.005
D-HR	GRS/U. Zagreb	Quab./Cub./Hyca	-0.019	-0.009	-0.009	-0.009
D	KWU	Panbox	-0.008	-0.005	-0.005	-0.005
F	EDF	Coccinelle	-0.001	+0.002		
F	Framatome	Cesar		+0.000		
GB	Nucl. Electric	Panther	-0.001	-0.001	-0.001	-0.001
I	ENEL	Quandry-En	-0.007	-0.010		
NL	ECN	Panther	-0.009	-0.004	-0.004	-0.004
RC	INER	Arotta-3D	-0.010	-0.020	-0.020	-0.020
USA	Studsvik	Simulate	+0.005	+0.002	+0.002	+0.002
		Average Bias	**-0.006**	**-0.005**	**-0.006**	**-0.006**
		Standard Deviation	**0.007**	**0.007**	**0.007**	**0.007**

6.2.4 Peak factor in axial layer 6 (B4)

Axial layer 6 is located at 108.7 cm above the bottom of the active core. Most of the results are included in a 1% range. The larger differences observed for INER are probably due to using a different normalisation scheme. This result was excluded from the statistics.

Table 11. Initial peak factor in axial layer 6

Country	Participant	Code	A	B	C	D
		Reference	**1.542**	**2.377**	**2.377**	**2.377**
B	Tractebel	Okapi	-0.007	-0.009	-0.009	-0.009
D-HR	GRS/U. Zagreb	Quab./Cub./Hyca	-0.022	-0.009	-0.009	-0.009
D	KWU	Panbox	-0.010	-0.006	-0.007	-0.006
F	EDF	Coccinelle	-0.003	-0.001		
F	Framatome	Cesar		+0.004		
GB	Nucl. Electric	Panther	-0.001	-0.001	-0.001	-0.001
I	ENEL	Quandry-En	-0.008	-0.012		
NL	ECN	Panther	-0.011	-0.005	-0.005	-0.005
RC	INER	Arotta-3D	*-0.320*	*-0.492*	*-0.492*	*-0.492*
USA	Studsvik	Simulate	+0.010	+0.010	+0.010	+ 0.010
		Average Bias	**-0.007**	**-0.003**	**-0.004**	**-0.003**
		Standard Deviation	**0.009**	**0.007**	**0.007**	**0.007**

6.2.5 Peak factor in axial layer 13 (B5)

Axial layer 13 is located at 318.7 cm above the bottom of the active core. Most of the results are included within a 1% range, with the same remark as above.

Table 12. Initial peak factor in axial layer 13

Country	Participant	Code	A	B	C	D
		Reference	**0.811**	**1.245**	**1.245**	**1.245**
B	Tractebel	Okapi	-0.001	-0.003	-0.003	-0.003
D-HR	GRS/U. Zagreb	Quab./Cub./Hyca	-0.015	-0.012	-0.012	-0.012
D	KWU	Panbox	-0.005	-0.001	-0.001	-0.001
F	EDF	Coccinelle	+0.002	+0.006		
F	Framatome	Cesar		+0.004		
GB	Nucl. Electric	Panther	-0.001	-0.001	-0.001	-0.001
I	ENEL	Quandry-En	-0.006	-0.007		
NL	ECN	Panther	-0.006	-0.003	-0.003	-0.003
RC	INER	Arotta-3D	*+0.397*	*+0.602*	*+0.602*	*+0.602*
USA	Studsvik	Simulate	-0.009	-0.019	-0.019	-0.019
		Average Bias	**-0.005**	**-0.004**	**-0.007**	**-0.007**
		Standard Deviation	**0.005**	**0.008**	**0.007**	**0.007**

6.2.6 Global (3-D) peak factor FQ (B6)

We observe here a broader dispersion of the results, and two groups can be identified:

- Quabox, Panbox, Panther, Quandry and Arotta are close to the reference.

- Okapi, Coccinelle, Cesar and Simulate obtain an about 10% higher FQ; the reason is that these codes give a local (reconstructed or nodal) maximum, while the other and the reference give the assembly maximum (see table 2 in § 4). In addition, the 1-D code Okapi is based on a factorisation method (2D*1D), that has a natural trend to increase the 3-D shape factor.

Appendix C shows the axial "envelope" profile (B6). The term "envelope" refers to the fact that the pellet that produces the maximum local power can possibly change along the vertical axis.

Table 13. Initial global (3-D) peak factor

Country	Participant	Code	A	B	C	D
		Reference	**1.880**	**2.886**	**2.886**	**2.886**
B	Tractebel	Okapi	+0.272	+0.130	+0.130	+0.130
D-HR	GRS/U. Zagreb	Quab./Cub./Hyca	-0.024	-0.005	-0.005	-0.005
D	**KWU**	**Panbox**	-0.013	-0.009	-0.009	-0.009
F	EDF	Coccinelle	+0.101	+0.196		
F	Framatome	Cesar		+0.184		
GB	Nucl. Electric	Panther	-0.001	-0.001	-0.001	-0.001
I	ENEL	Quandry-En	-0.010	-0.014		
NL	ECN	Panther	-0.013	-0.006	-0.006	-0.006
RC	INER	Arotta-3D	-0.017	-0.032	-0.032	-0.032
USA	Studsvik	Simulate	+0.120	+0.251	+0.251	+0.251
		Average Bias	**+0.046**	**+0.069**	**+0.047**	**+0.047**

		Standard Deviation	**0.101**	**0.108**	**0.105**	**0.105**

The output data set provides another way to get the global shape factor FQ, by comparing the initial power in hot pellet (D1 at t=0s) to the core average (10^{-13} nominal power). We would expect a slightly higher value than from B6 "envelope" profile, because this profile is given only for 16 axial meshes, while D1 should use the finest available meshing. Radially, Okapi, Coccinelle, Cesar and Simulate give a local or nodal maximum in both B6 and D1, while Panbox gives the assembly maximum in B6 and a local maximum in D1. Panbox provides therefore a basis for comparing the results of these four codes to the reference solution.

The comparison is shown in Table 14. In some cases, D1 gave a lower value than B6, but we found from the detailed data files that in these cases, the solution for item D1 was not numerically stable at this (very low) initial power. These values appear in italic in the table.

Table 14. Consistency check on initial FQ, based on items B6 and D1

Country	Participant	Code	A	B	C	D
	Reference	**B6 (maximum)** **D1 (time=0)**	**1.880** **1.994**	**2.886** **3.117**	**2.886** **3.117**	**2.886** **3.117**
B	Tractebel	Okapi	2.152 2.173	3.015 3.044	3.015 3.044	3.015 3.044
D-HR	GRS/U. Zagreb	Quab./Cub./Hyca	1.856 *1.856*	2.880 *2.953*	2.880 *2.953*	2.880 *2.970*
D	KWU	Panbox	1.867 2.114	2.876 3.140	2.876 3.139	2.876 3.140
F	EDF	Coccinelle	1.981 1.999	3.082 3.106	--- ---	--- ---
F	Framatome	Cesar	--- ---	3.070 3.068	--- ---	--- ---
GB	Nucl. Electric	Panther	1.879 1.941	2.885 2.939	2.885 2.939	2.885 2.939
I	ENEL	Quandry-En	1.870 *0.1512*	2.871 *0.2702*	--- ---	--- ---
NL	ECN	Panther	1.866 1.867	2.880 2.880	2.880 2.880	2.880 2.880
RC	INER	Arotta-3D	1.863 1.857	2.853 2.843	2.853 2.843	2.853 2.843
USA	Studsvik	Simulate	2.000 *1.803*	3.137 *2.985*	3.137 *1.958*	3.137 *2.985*

6.3 Transient evolution (core average)

Appendix 2 shows the evolution of the four parameters selected for the analysis. The following tables intend to provide a synoptic view of all cases and participants, including an evaluation of the deviation with respect to the reference solution.

6.3.1 General remarks about the analysed cases

- In **Case A**, a first power peak occurs, under the trigger level (35 %), followed by a relatively slow power increase. The SCRAM is affected by a 0.6 s delay, so that the maximum fission power is slightly above this level. Arotta-3D obtains a different power evolution, with a high,

but narrow power surge (50 %). This result (displayed in italic) is therefore excluded from all the statistics for Case A. It is interesting to note that ENEL reported that they observed the same problem with Quandry when running the problem with a too coarse meshing. The problem disappeared after refining the meshing.

- In **Case B**, a higher reactivity is inserted, resulting in a fast power surge, with only one peak; the main factor limiting the power is the Doppler feedback, because of the SCRAM delay.

- **Case C** was designed to cancel the possible influence of the T&H heat transfer correlation, by imposing a constant heat transfer coefficient. All other data are the same as for Case B. The differences are very small, as shown in the tables. We therefore omitted the plots for Case C in Appendix B.

- **Case D** behaves similarly to Cases B and C.

6.3.2 Maximum fission power (C1)

The peak power is given as a fraction of the nominal power. The very good agreement obtained for Case A is due to the fact that after a first power burst, the power continues to increase, slowly, up to the 35% scram level. The maximum is therefore always slightly higher than 35%.

For the other cases, the power burst is sharper, and larger deviations are observed, but one should remember that the value of the peak is less important than its time integral (i.e. the released energy). The fuel Doppler temperature (C4), hot pellet fuel enthalpy (D5) and hot pellet centreline temperature (D6) provide a better way to determine the quality of the results.

It should be noted that the maximum power can be sensitive to the size of the time steps used.

Appendix B shows that the general evolution is almost the same for all the participants, except for Arotta in Case A, as already mentioned.

Table 15. Maximum fission power (C1)

Country	Participant	Code	A	B	C	D
		Reference	**0.3556**	**1.3480**	**1.3423**	**0.9685**
B	Tractebel	Okapi	+0.0%	+25.7%	+26.1%	+31.4%
D-HR	GRS/U. Zagreb	Quab./Cub./Hyca	-0.2%	-25.2%	-24.8%	+30.5%
D	KWU	Panbox	-0.1%	+13.0%	+13.7%	+6.2%
F	EDF	Coccinelle	+0.3%	+22.2%		
F	Framatome	Cesar		-4.5%		
GB	Nucl. Electric	Panther	-0.1%	-2.6%	-2.9%	+6.6%
I	ENEL	Quandry-En	+0.0%	-13.2%		
NL	ECN	Panther	+0.3%	+32.9%	+33.9%	+5.0%
RC	INER	Arotta-3D	*+30.8%*	-29.4%	-28.7%	+36.4%
USA	Studsvik	Simulate	+0.6%	-36.7%	-36.1%	-23.2%
		Average Bias	**+0.1%**	**-1.8%**	**-2.7%**	**+13.3%**
		Standard Deviation	**0.3%**	**24.5%**	**28.0%**	**21.0%**

6.3.3 Time of maximum fission power (C1)

The plots given in Appendix B provide a better view of the evolution. From Table 16, we observe that:

- OKAPI is always in advance, by a few seconds;
- Panbox, Coccinelle, and Panther (with standard meshing) anticipate, by 1 s or less;
- Cesar and Simulate are slightly late, by a fraction of a second;
- Quabox and Quandry obtain the peak later, by up to 2 s.

This result is however not very important from a safety point of view.

Table 16. Time(s) of maximum fission power (C1)

Country	Participant	Code	A	B	C	D
		Reference	**82.14**	**34.30**	**34.30**	**39.40**
B	Tractebel	Okapi	-2.19	-2.57	-2.57	-3.68
D-HR	GRS/U. Zagreb	Quab./Cub./Hyca	+1.61	+0.73	+0.73	+0.35
D	KWU	Panbox	-1.14	-0.33	-0.32	-0.77
F	EDF	Coccinelle	-0.54	-0.12		
F	Framatome	Cesar		+0.65		
GB	Nucl. Electric	Panther	-0.34	-0.08	-0.08	-0.04
I	ENEL	Quandry-En	+2.00	+0.41		
NL	ECN	Panther	-0.16	-0.17	-0.17	-0.92
RC	INER	Arotta-3D	*-5.55*	+2.26	+2.26	+2.15
USA	Studsvik	Simulate	+0.56	+0.14	+0.14	+0.25
		Average Bias	**-0.03**	**+0.09**	**-0.00**	**-0.38**
		Standard Deviation	**1.39**	**1.20**	**1.44**	**1.77**

6.3.4 Maximum of coolant heating (C2)

The coolant heating is given here as a fraction of the nominal power. This result corresponds more or less to the temperature excursion, or the integral of the fission power. Coccinelle cannot output this result and is omitted in the table.

Most of the codes, including the ECN Panther solution, obtain a value higher than the reference (obtained by Panther with refined meshing and time steps).

Table 17. Maximum of the coolant heating (C2)

Country	Participant	Code	A	B	C	D
		Reference	**0.2951**	**0.1379**	**0.1367**	**0.1253**
B	Tractebel	Okapi	+10.3%	+28.8%	+30.2%	+30.4%
D-HR	GRS/U. Zagreb	Quab./Cub./Hyca	+28.5%	+29.3%	+29.7%	+54.0%
D	KWU	Panbox	+5.7%	+20.9%	+21.7%	+17.6%
F	EDF	Coccinelle				
F	Framatome	Cesar		-1.6%		
GB	Nucl. Electric	Panther	+1.5%	+2.1%	-0.1%	+2.9%
I	ENEL	Quandry-En	+10.8%	+12.2%		
NL	ECN	Panther	+8.3%	+26.0%	+26.9%	+17.5%
RC	INER	Arotta-3D	*-53.1%*	-3.7%	-4.4%	+16.7%
USA	Studsvik	Simulate	+11.7%	+13.0%	+13.3%	+21.4%
		Average Bias	**+11.0%**	**+14.1%**	**+16.8%**	**+22.9%**
		Standard Deviation	**8.5%**	**13.0%**	**14.3%**	**15.9%**

6.3.5 Maximum of coolant outlet temperature (C3)

This result is the integral of the coolant heating. It is observed that the temperature increase at outlet is limited to about 10°C in all cases. The same remark as for C2 above applies here: most of the codes, including Panther, obtain higher value than the reference solution, except for Quabox and the Nuclear electric Panther solution.

Table 18. Maximum coolant outlet temperature (C3), in °C

Country	Participant	Code	A	B	C	D
		Reference	**295.3**	**290.5**	**290.4**	**290.0**
B	Tractebel	Okapi	+3.5	+1.7	+1.8	+1.7
D-HR	GRS/U. Zagreb	Quab./Cub./Hyca	-1.1	-1.4	-1.4	-0.5
D	KWU	Panbox	+3.1	+1.8	+1.8	+1.9
F	EDF	Coccinelle	+3.5	+2.2		
F	Framatome	Cesar		+1.0		
GB	Nucl. Electric	Panther	-2.1	-0.4	-0.5	-0.3
I	ENEL	Quandry-En	+3.7	+1.1		
NL	ECN	Panther	+0.2	+0.8	+0.9	+0.3
RC	INER	Arotta-3D	*-2.4*	+3.0	+3.0	+4.3
USA	Studsvik	Simulate	+4.0	+1.3	+1.3	+1.7
		Average Bias	**+1.9**	**+1.1**	**+1.0**	**+1.3**
		Standard Deviation	**2.5**	**1.3**	**1.5**	**1.7**

6.3.6 Maximum of fuel Doppler temperature (C4)

This result is an image of the Doppler feedback, the main factor limiting the peak power in Cases B, C, D. Most of the codes, including Panther, obtain a temperature a few degrees above the reference solution in many cases.

Table 19. Maximum fuel Doppler temperature (C4), in °C

Country	Participant	Code	A	B	C	D
		Reference	**358.7**	**315.2**	**315.4**	**312.6**
B	Tractebel	Okapi	+1.9	+4.2	+3.9	+4.0
D-HR	GRS/U. Zagreb	Quab./Cub./Hyca	+1.8	-0.5	-0.4	+5.2
D	KWU	Panbox	-1.2	+3.6	+3.6	+2.3
F	EDF	Coccinelle	-0.1	+4.1		
F	Framatome	Cesar		+3.8		
GB	Nucl. Electric	Panther	-0.4	+0.3	-0.1	+0.8
I	ENEL	Quandry-En	+0.6	-1.3		
NL	ECN	Panther	-0.9	+3.5	+3.5	+0.8
RC	INER	Arotta-3D	*-33.9*	+9.3	+9.4	+15.8
USA	Studsvik	Simulate	+2.0	+0.5	+0.5	+2.5
		Average Bias	**+0.5**	**+2.7**	**+2.9**	**+4.5**
		Standard Deviation	**1.3**	**3.1**	**3.4**	**5.2**

6.4 Transient evolution (hot pellet)

6.4.1 Introduction

The "hot pellet" is defined as the pellet that produces the higher fission power. The location of this pellet can move during the transient, as well in radial as in axial position. The "hot channel" is the T&H channel corresponding to the assembly where the "hot pellet" is located.

Although 1-D and 3-D codes provide hot pellet and hot channel results, the method for determining them is different. While 3-D codes uses assembly T&H channels, 1-D code "OKAPI" reconstructs a "hot channel" using the envelope of the radial peak power along the vertical axis; this method has a natural trend to overestimate the power.

Appendix B shows the evolution of the seven parameters selected for the analysis. The following tables intend to provide a synoptic view of all cases and participants, including an evaluation of the deviation with respect to the reference solution.

In general, one can say that the results in the hot pellet are more spread than those obtained for the core average. In most of the cases, the definition of the hot pellet in itself is the source of the problem, as explained in § 6.2.6 and Table 14 for steady state.

6.4.2 Maximum fission power in hot pellet w/r to nominal power (D1)

The evolution (see Appendix B) is almost the same for all codes (except for Arotta in Case A). The time of the maximum power is almost the same as for the core average power. Table 20 shows the reference solution, as a fraction of the core average nominal power, and the relative deviations.

- In Case A, although the maximum power level in the core is slightly above 0.35 nominal for all participants, larger differences (up to 7%) are observed for the local maximum, with three "families" of results:
  - Panther (N.E.) and Coccinelle are close to the reference (deviation < 1%);
  - Okapi, Panbox, and Simulate overestimate the power (about +8%);
  - Quabox, Quandry, Panther (NL) underestimate the power (a few %);
  - Arotta obtains a different evolution and is not included in the statistics.
- In Case B (and C), the deviations are larger, and we have again three "families" of results, but not the same as in Case A:
  - Panbox, Cesar, Panther (GB) are fairly close to the reference (deviation < 10%);
  - Okapi, Coccinelle, and Panther (NL) overestimate the power (about +25%);
  - Quabox, Quandry, and Simulate underestimate the power (about -35%).
- Similar conclusions are obtained for Case D, but in this case:
  - the two Panther solutions are relatively close to the reference (deviation < 20%);
  - Okapi, Quabox, Panbox and Arotta overestimate the power (+20-40%);
  - Simulate underestimates the power (about -25%).

Actually, no general conclusion can be drawn concerning the under or overestimation trend of the codes.

Case A should be considered separately, as the core average power is almost the same for most of the participants, and consequently the deviations emerge mainly from the peaking factor (FQ).

For Cases B, C, and D, we observe that:

- Okapi, Panbox, and Coccinelle always obtain a higher power than the reference;
- Cesar, Quandry, and Simulate underestimate the power.

From a safety point of view, the maximum power in itself is less important than its integral, i.e. the released energy.

Table 20. Maximum fission power in hot pellet w/r to nominal power (D1)

Country	Participant	Code	A	B	C	D
		Reference	**0.8771**	**6.0016**	**5.9833**	**3.9428**
B	Tractebel	Okapi	+8.9%	+29.2%	+29.5%	+42.0%
D-HR	GRS/U. Zagreb	Quab./Cub./Hyca	-4.3%	-37.4%	-37.1%	+17.4%
D	KWU	Panbox	+8.0%	+0.5%	+1.8%	+20.0%
F	EDF	Coccinelle	+1.1%	+21.2%		
F	Framatome	Cesar		-6.7%		
GB	Nucl. Electric	Panther	-0.9%	-7.2%	-7.7%	+5.3%
I	ENEL	Quandry-En	-4.5%	-26.3%		
NL	ECN	Panther	-2.9%	+17.0%	+17.6%	-4.1%
RC	INER	Arotta-3D	*+24.9%*	-39.7%	-39.2%	+23.3%
USA	Studsvik	Simulate	+7.8%	-36.5%	-36.0%	-25.3%
		Average Bias	**+1.7%**	**-8.6%**	**-10.2%**	**+11.2%**
		Standard Deviation	**5.8%**	**25.7%**	**28.1%**	**21.6%**

6.4.3 Maximum coolant heating in hot pellet w/r to average nominal power (D2)

The coolant heating is given here as a fraction of the core average nominal power. This result corresponds more or less to the hot pellet temperature excursion, or the integral of the fission power. Coccinelle and Arotta cannot output this result and are therefore omitted here.

It is interesting to observe that although the peak power is much higher in Cases B, C, D than in Case A, the coolant heating remains around 70% in all four cases.

The results from Quandry are 50% lower than the other results, so that they were excluded from the statistics. Since the fission power evolution obtained by Quandry is similar to the other one, we think that this deviation could be due to a confusion between hot pellet and core average.

Table 21. Maximum coolant heating in hot pellet w/r to average nominal power (D2)

Country	Participant	Code	A	B	C	D
		Reference	**0.7575**	**0.6816**	**0.6789**	**0.5760**
B	Tractebel	Okapi	+14.2%	+13.7%	+14.2%	+20.3%
D-HR	GRS/U. Zagreb	Quab./Cub./Hyca	-2.0%	-16.4%	-16.6%	+5.4%
D	KWU	Panbox	-2.4%	+2.3%	+2.3%	-1.5%
F	EDF	Coccinelle				
F	Framatome	Cesar		-9.0%		
GB	Nucl. Electric	Panther	-0.7%	-1.3%	-2.1%	+2.2%
I	ENEL	Quandry-En	*-49.9%*	*-53.8%*		
NL	ECN	Panther	+0.6%	+9.5%	+9.5%	+2.6%
RC	INER	Arotta-3D				
USA	Studsvik	Simulate	+14.8%	+5.6%	+5.2%	+15.7%
		Average Bias	**+4.1%**	**+0.6%**	**+2.1%**	**+7.5%**

		Standard Deviation	**8.1%**	**10.5%**	**10.8%**	**8.6%**

6.4.4 Maximum coolant temperature at outlet of hot channel (D3)

The power excursion is relatively small in Case A and very fast in other cases, so the temperature does not increase very much in the hot channel (16°C in Case A). The heating is underestimated by most of the participants, except for Okapi, Coccinelle, and Panther (NL).

Table 22. Maximum coolant temperature at outlet of hot channel (D3), in °C

Country	Participant	Code	A	B	C	D
		Reference	**302.0**	**297.2**	**297.1**	**296.0**
B	Tractebel	Okapi	+1.1	+0.2	+0.3	+0.3
D-HR	GRS/U. Zagreb	Quab./Cub./Hyca	-2.2	-3.0	-3.0	-0.9
D	KWU	Panbox	-1.3	-0.1	-0.0	-0.3
F	EDF	Coccinelle	-0.8	+0.4		
F	Framatome	Cesar		-1.8		
GB	Nucl. Electric	Panther	-3.7	-1.6	-1.7	-1.2
I	ENEL	Quandry-En	-0.9	-1.8		
NL	ECN	Panther	-0.9	+0.4	+0.4	-0.3
RC	INER	Arotta-3D	*-9.5*	-2.1	-2.1	+0.0
USA	Studsvik	Simulate	-1.6	-1.2	-1.2	-0.5
		Average Bias	**-1.3**	**-1.1**	**-1.0**	**-0.4**
		Standard Deviation	**1.4**	**1.2**	**1.3**	**0.5**

6.4.5 Maximum heat exchange coefficient between cladding and moderator in hot pellet (D4)

The heat exchange coefficients obtained by the participants does not differ very much: a few %, or less, in most of the cases. In Case C, the value is imposed. The slight variation observed with Panbox is an effect of the implementation of this specification in the code.

Table 23. Maximum cladding/moderator heat exchange coefficient in hot pellet (D4)

Country	Participant	Code	A	B	C	D
		Reference (W/m2/°C)	**33407**	**33335**	**30000**	**33253**
B	Tractebel	Okapi	+2.2%	+2.7%	-0.0%	+2.6%
D-HR	GRS/U. Zagreb	Quab./Cub./Hyca	+3.0%	+3.1%	-0.0%	+3.4%
D	KWU	Panbox	+0.4%	+0.4%	*+0.3%*	+1.1%
F	EDF	Coccinelle	+1.6%	+0.5%		
F	Framatome	Cesar		-1.8%		
GB	Nucl. Electric	Panther	-0.1%	-0.1%	-0.0%	-0.0%
I	ENEL	Quandry-En	+1.1%	+1.0%		
NL	ECN	Panther	-0.2%	+0.1%	-0.0%	-0.1%
RC	INER	Arotta-3D				
USA	Studsvik	Simulate	+2.5%	+2.7%	-0.0%	+2.9%
		Average Bias	**+1.3%**	**+0.9%**	**none**	**+1.7%**
		Standard Deviation	**1.2%**	**1.6%**	**none**	**1.5%**

6.4.6 Minimum heat exchange coefficient between cladding and moderator in hot pellet (D4)

We also present the minimum value of this coefficient to give an idea of the variation range. This range remains very limited. This explains why Case C is very close to Case B, showing very little influence of the heat exchange correlation.

Table 24. Minimum cladding/moderator heat exchange coefficient in hot pellet (D4)

Country	Participant	Code	A	B	C	D
		Reference (W/m2/°C)	**32569**	**32569**	**30000**	**32569**
B	Tractebel	Okapi	+0.1%	-3.6%	-0.0%	-3.6%
D-HR	GRS/U. Zagreb	Quab./Cub./Hyca	+4.7%	+4.7%	-0.0%	+4.7%
D	KWU	Panbox	+1.3%	+0.8%	*-0.8%*	+1.9%
F	EDF	Coccinelle	+2.4%	+2.4%		
F	Framatome	Cesar		+0.1%		
GB	Nucl. Electric	Panther	-0.0%	-0.0%	-0.0%	-0.0%
I	ENEL	Quandry-En	+2.5%	+2.5%		
NL	ECN	Panther	-0.0%	-0.0%	-0.0%	-0.0%
RC	INER	Arotta-3D				
USA	Studsvik	Simulate	+5.1%	+5.1%	-0.0%	+5.1%
		Average Bias	**+2.0%**	**+1.3%**	**none**	**+1.4%**
		Standard Deviation	**2.1%**	**2.7%**	**none**	**3.3%**

6.4.7 Maximum fuel enthalpy in hot pellet (D5)

From a safety point of view, this result is important to evaluate the severity of the accident.

The initial value of the enthalpy should be 125868 J/Kg. Actually, a few participants took a different temperature as reference. We evaluate here the enthalpy increase, cancelling any initial difference. The deviations are calculated in % of the enthalpy increase obtained in the reference solution.

The standard deviation is about 10%:

- Okapi and, at a lower level Panbox overestimate the heating of the hot pellet;
- Quabox (except for Case D), Panther (GB and NL), and Quandry underestimate it.

Table 25. Maximum fuel enthalpy injected in hot pellet (D5)

Country	Participant	Code	A	B	C	D
		Reference (J/Kg)	**61662**	**45882**	**46121**	**38251**
B	Tractebel	Okapi	+12.4%	+8.1%	+7.3%	+14.7%
D-HR	GRS/U. Zagreb	Quab./Cub./Hyca	-5.0%	-22.2%	-21.9%	+2.0%
D	KWU	Panbox	+0.7%	+2.6%	+2.7%	+2.9%
F	EDF	Coccinelle				
F	Framatome	Cesar		-15.0%		
GB	Nucl. Electric	Panther	-2.2%	-5.9%	-7.1%	-0.7%
I	ENEL	Quandry-En	-3.3%	-20.2%		
NL	ECN	Panther	-4.8%	-0.9%	-0.9%	-5.9%
RC	INER	Arotta-3D	*-59.9%*	-13.9%	-13.5%	+10.8%
USA	Studsvik	Simulate	+8.5%	-1.4%	-1.5%	+9.1%
		Average Bias	**+0.9%**	**-7.6%**	**-5.0%**	**+4.7%**
		Standard Deviation	**6.9%**	**10.6%**	**10.0%**	**7.2%**

6.4.8 Time of maximum fuel enthalpy in hot pellet (D5)

Table 26. Time(s) of maximum fuel enthalpy in hot pellet (D5)

Country	Participant	Code	A	B	C	D
		Reference	**82.19**	**34.85**	**34.85**	**39.95**
B	Tractebel	Okapi	-2.19	-2.58	-2.57	-3.69
D-HR	GRS/U. Zagreb	Quab./Cub./Hyca	+1.61	+0.72	+0.74	+0.34
D	KWU	Panbox	-1.09	-0.35	-0.35	-0.84
F	EDF	Coccinelle				
F	Framatome	Cesar		+0.65		
GB	Nucl. Electric	Panther	-0.34	-0.06	-0.08	-0.03
I	ENEL	Quandry-En	+2.00	+0.39		
NL	ECN	Panther	-0.15	-0.17	-0.17	-0.92
RC	INER	Arotta-3D	-5.18	+2.31	+2.31	+2.16
USA	Studsvik	Simulate	+0.55	+0.20	+0.20	+0.36
		Average Bias	**-0.60**	**+0.12**	**+0.01**	**-0.37**
		Standard Deviation	**2.30**	**1.28**	**1.45**	**1.78**

6.4.9 Maximum fuel temperature at centreline of hot pellet (D6)

This is another important result to evaluate the severity of the accident. We would expect similar conclusions as for the enthalpy. However, it is not the case for all codes. The differences are probably due to the pellet models.

In general, the trend is consistent with the definitions chosen for the hot pellet (see Table 2). Okapi, Panbox and Simulate use a finer intra assembly power distribution and obtain higher temperatures for most of the cases.

We give here also the reference solution obtained with one T&H channel per fuel element (as specified) instead of 3×3 channels; we see that the bias is then reduced.

Table 27. Maximum fuel temperature at centreline in hot pellet (D6), in °C

Country	Participant	Code	A	B	C	D
		Reference (1 channel/F.E)	**631.8 (-2.2)**	**478.2 (+4.8)**	**479.0 (+4.8)**	**451.4 (+5.5)**
B	Tractebel	Okapi	+57.3	+46.9	+45.9	+47.3
D-HR	GRS/U. Zagreb	Quab./Cub./Hyca	-26.7	-28.2	-27.8	+16.9
D	KWU	Panbox	-14.8	+15.8	+16.1	+14.8
F	EDF	Coccinelle	-3.2	+32.6		
F	Framatome	Cesar		-13.1		
GB	Nucl. Electric	Panther	-2.0	+2.0	-0.8	+4.9
I	ENEL	Quandry-En	+3.3	-20.6		
NL	ECN	Panther	-6.3	+20.9	+20.8	+4.7
RC	INER	Arotta-3D				
USA	Studsvik	Simulate	+53.2	+33.0	+32.4	+44.6
		Average Bias (1 channel / F.E.)	**+7.6 (+9.8)**	**+10.0 (+5.2)**	**+14.4 (+9.6)**	**+22.2 (+16.7)**
		Standard Deviation	**30.8**	**26.3**	**26.0**	**19.1**

6.4.10 Maximum hot pellet cladding outer surface temperature (D7)

The heating at the outer surface of the cladding remains very limited at this point (about 20°C). Most of the participants obtain lower values than the reference solution, except for Okapi and Cesar. Simulate obtains the lowest temperatures (6-9°C below the reference)

Table 28. Maximum hot pellet cladding outer surface temperature (D7), in °C

Country	Participant	Code	A	B	C	D
		Reference	**308.2**	**303.6**	**304.7**	**301.3**
B	Tractebel	Okapi	+4.3	+4.5	+3.1	+4.2
D-HR	GRS/U. Zagreb	Quab./Cub./Hyca	-3.5	-4.9	-4.8	-1.2
D	KWU	Panbox	-1.9	-0.7	-0.5	-1.4
F	EDF	Coccinelle	-2.1	+0.4		
F	Framatome	Cesar		+3.7		
GB	Nucl. Electric	Panther	-0.5	-1.0	-1.1	-0.1
I	ENEL	Quandry-En	-0.8	-1.6		
NL	ECN	Panther	-1.0	+0.5	+0.5	-0.7
RC	INER	Arotta-3D				
USA	Studsvik	Simulate	-7.8	-7.6	-8.8	-5.8
		Average Bias	**-1.7**	**-0.8**	**-1.9**	**-0.8**
		Standard Deviation	**3.4**	**3.8**	**4.2**	**3.2**

6.5 Snapshot at time of maximum power

The following results have been compared: average axial and radial power distributions, axial, radial and 3-D shape factors (Fxy, Fz and FQ), envelope axial power distribution, and “slices” of radial power distribution. The conclusions are mainly the same as at the initial steady state. Appendices C and D show the axial and radial power profiles, while the following tables give a comparison of the shape factors.

6.5.1 Maximum fission power (E1)

This result has already been given in § 6.3.2.

6.5.2 Axial peak factor Fz (E2)

Appendix C shows that the radially averaged axial profiles are very similar, except in the transition region, just below the edge of the moving rods. A few seconds separate the participants so that the rods are not exactly at the same position (4 s = 5 steps). The method for taking into account nodes with partially inserted rods plays also a role.

It should be noted that Fz is derived here from 16 axial nodes (nodal maximum). This leads to a slight underestimation of Fz, but should affect the participants' solutions as well as the reference solutions.

With respect to the latter, the differences are small in most of the cases:

- Panbox, Cesar, Panther have less than 2% deviation;
- Quabox, Coccinelle, Arotta and Simulate underestimate Fz (up to -11%);
- Okapi overestimates Fz by up to 9%.

Table 29. Axial peak factor Fz at time of maximum fission power (E2)

Country	Participant	Code	A	B	C	D
		Reference	**1.985**	**2.437**	**2.435**	**2.325**
B	Tractebel	Okapi	+0.018	+0.090	+0.092	+0.090
D-HR	GRS/U. Zagreb	Quab./Cub./Hyca	-0.021	-0.079	-0.076	-0.038
D	KWU	Panbox	-0.008	-0.012	-0.010	+0.014
F	EDF	Coccinelle	-0.018	-0.105		
F	Framatome	Cesar		-0.011		
GB	Nucl. Electric	Panther	+0.001	-0.003	-0.006	+0.004
I	ENEL	Quandry-En	-0.029	-0.089		
NL	ECN	Panther	+0.002	+0.010	+0.012	+0.015
RC	INER	Arotta-3D	-0.035	-0.109	-0.108	-0.047
USA	Studsvik	Simulate	-0.002	-0.045	-0.044	-0.032
		Average Bias	**-0.010**	**-0.035**	**-0.020**	**+0.001**
		Standard Deviation	**0.017**	**0.063**	**0.065**	**0.047**

6.5.3 Radial peak factor Fxy (E3)

Appendix D shows that, except for Quabox in Case A, the agreement on the axially averaged radial profiles is good, although less than for steady state conditions. It should be noted that Fxy is derived here from the assembly averaged power distribution (assembly maximum).

Table 30. Radial peak factor Fxy at time of maximum fission power (E3)

Country	Participant	Code	A	B	C	D
		Reference	**1.195**	**1.751**	**1.751**	**1.715**
B	Tractebel	Okapi	+0.005	-0.008	-0.008	+0.033
D-HR	GRS/U. Zagreb	Quab./Cub./Hyca	-0.022	-0.045	-0.045	-0.008
D	KWU	Panbox	-0.005	-0.016	-0.016	-0.005
F	EDF	Coccinelle	+0.001	+0.009		
F	Framatome	Cesar		+0.007		
GB	Nucl. Electric	Panther	-0.000	-0.001	-0.002	-0.001
I	ENEL	Quandry-En	-0.009	-0.032		
NL	ECN	Panther	-0.007	-0.022	-0.022	-0.006
RC	INER	Arotta-3D	+0.004	-0.016	-0.016	-0.013
USA	Studsvik	Simulate	+0.003	+0.010	+0.010	+0.004
		Average Bias	**-0.003**	**-0.012**	**-0.014**	**+0.001**
		Standard Deviation	**0.009**	**0.018**	**0.017**	**0.015**

6.5.4 Radial peak in axial layer 6 (E4)

Axial layer 6 is located at 108.7 cm above the bottom of the active core and therefore sensitive to the position of the control rods, thus to the timing of the power maximum.

The agreement is good, except for Arotta (normalisation problem), and Okapi in Case D. These results were excluded from the statistics.

Table 31. Radial peak in axial layer 6 at time of maximum fission power (E4)

Country	Participant	Code	A	B	C	D
		Reference	**2.395**	**3.053**	**3.051**	**3.120**
B	Tractebel	Okapi	+0.044	-0.063	-0.061	*-0.216*
D-HR	GRS/U. Zagreb	Quab./Cub./Hyca	-0.033	+0.002	+0.006	+0.020
D	KWU	Panbox	-0.008	-0.029	-0.027	-0.002
F	EDF	Coccinelle	-0.027	+0.078		
F	Framatome	Cesar		+0.015		
GB	Nucl. Electric	Panther	+0.001	-0.007	-0.011	+0.001
I	ENEL	Quandry-En	-0.040	-0.006		
NL	ECN	Panther	-0.003	-0.024	-0.022	-0.003
RC	INER	Arotta-3D	*-0.231*	*+0.748*	*+0.750*	*+0.559*
USA	Studsvik	Simulate	-0.004	+0.043	+0.045	+0.043
		Average Bias	**-0.009**	**+0.001**	**-0.012**	**+0.012**
		Standard Deviation	**0.026**	**0.041**	**0.035**	**0.020**

6.5.5 Radial peak in axial layer 13 (E5)

Axial layer 13 is located at 318.7 cm above the bottom of the active core. Except for Arotta (normalisation problem), the results are good. It is observed, however that for Case A, all the solutions, including the two Panther solutions, give a value 3% lower than the reference.

Table 32. Radial peak in axial layer 13 at time of maximum fission power (E5)

Country	Participant	Code	A	B	C	D
		Reference	**0.272**	**0.322**	**0.323**	**0.330**
B	Tractebel	Okapi	-0.010	-0.026	-0.027	-0.023
D-HR	GRS/U. Zagreb	Quab./Cub./Hyca	+0.009	+0.003	+0.001	-0.009
D	KWU	Panbox	+0.006	+0.006	+0.005	-0.002
F	EDF	Coccinelle	+0.007	+0.015		
F	Framatome	Cesar		+0.004		
GB	Nucl. Electric	Panther	+0.000	+0.002	+0.004	-0.002
I	ENEL	Quandry-En	+0.005	+0.006		
NL	ECN	Panther	+0.001	-0.003	-0.004	-0.001
RC	INER	Arotta-3D	*+0.249*	*+0.220*	*+0.219*	*+0.208*
USA	Studsvik	Simulate	+0.001	+0.005	+0.004	-0.001
		Average Bias	**+0.002**	**+0.001**	**-0.003**	**-0.006**
		Standard Deviation	**0.006**	**0.011**	**0.012**	**0.009**

6.5.6 Global (3-D) peak factor FQ (E6)

Comparing the differences observed for FQ to those obtained from the radial and axial assembly maximum, one can conclude that the definition of the hot pellet and the intra assembly power profile model are the main causes of the discrepancies observed.

Table 33. Global (3-D) peak factor FQ at time of maximum fission power (E6)

Country	Participant	Code	A	B	C	D
		Reference	**2.395**	**3.967**	**3.964**	**3.718**
B	Tractebel	Okapi	+0.274	+0.390	+0.393	+0.783
D-HR	GRS/U. Zagreb	Quab./Cub./Hyca	-0.030	-0.225	-0.217	-0.031
D	KWU	Panbox	-0.008	-0.083	-0.078	-0.005
F	EDF	Coccinelle	+0.048	+0.120		
F	Framatome	Cesar		+0.384		
GB	Nucl. Electric	Panther	+0.001	-0.012	-0.018	+0.003
I	ENEL	Quandry-En	-0.040	-0.189		
NL	ECN	Panther	-0.003	-0.058	-0.054	-0.006
RC	INER	Arotta-3D	-0.040	-0.167	-0.163	-0.039
USA	Studsvik	Simulate	+0.115	+0.232	+0.236	+0.296
		Average Bias	**+0.035**	**+0.039**	**+0.014**	**+0.143**
		Standard Deviation	**0.102**	**0.230**	**0.221**	**0.306**

REFERENCES

[1] H. Finnemann, A. Galati, *NEACRP 3-D LWR Core Transient Benchmark Final Specifications*, NEACRP-L-335, Rev. 1 (Jan. 1992).

[2] R. Fraikin, Ph. Maes, M. Mélice, *NEACRP 3-D/1-D PWR Core Transient Benchmark on Uncontrolled Withdrawal of Control Rods at Zero Power Proposal*, NEA 3D-LWR Benchmark Specialists Meeting, Paris (Sep. 1992).

[3] H. Finnemann, H. Bauer, A. Galati, R. Martinelli, *Results of LWR Core Transient Benchmarks*, Joint International Conference on Mathematical Methods and Supercomputing in Nuclear Applications, Karlsruhe, p. 243-258 (April 1993).

[4] R. Fraikin, H. Finnemann, *NEA-NSC 3-D/1-D PWR Core Transient Benchmark: Uncontrolled Withdrawal of Control Rods at Zero Power – Final Specifications,* OECD Nuclear Energy Agency, NEA/NSC/ DOC(93)9 (Sep. 1993).

[5] H. Finnemann, H. Bauer, A. Galati, R. Martinelli, *Results of LWR Core Transients Benchmarks,* NEA/NSC/DOC(93)25 (Oct. 1993).

[6] J.C. Kuijper, *Panther Solution to the NEA-NSC 3-D PWR Core Transient Benchmark: Uncontrolled Withdrawal of Control Rods at Zero Power*, ECN-R-94-023 (Oct. 1994).

[7] R. Fraikin, *NEA-NSC PWR Benchmarks Review,* Specialists Meeting on LWR Core Transient Benchmarks NEA/NSC, Paris (May 1995).

[8] Ph. Brohan, *PANTHER Results for the NEA-NSC 3-D PWR Core Transient Benchmark,* Specialists Meeting on LWR Core Transient Benchmarks NEA/NSC, Paris, 10-12 May 1995.

[9] M. Mélice, R. Fraikin, Ph. Maes, Ch. Schneidesch, *NEA-NSC PWR Core Transient Benchmark on Rod Withdrawal from Zero Power: Axial Meshing Sensitivity Study*, Specialists Meeting on LWR Core Transient Benchmarks, NEA/NSC, Paris (May 1995).

[10] J. Kuijper, *PANTHER Solution to the NEA-NSC 3-D PWR Core Transient Benchmark on Uncontrolled Withdrawal of Control Rods at Zero Power,* Specialists Meeting on LWR Core Transient Benchmarks NEA/NSC, Paris, 10-12 May 1995.

[11] M. Pétiard, *NEA PWR Core Transient Benchmark on Uncontrolled Withdrawal of Control Rods at Zero Power, Framatome Results,* Specialists Meeting on LWR Core Transient Benchmarks NEA/NSC, Paris, 10-12 May 1995.

[12] G. Alloggio, E. Brega, *Results of Quandry-En Calculations, Cases A-B,* Specialists Meeting on LWR Core Transient Benchmarks NEA/NSC, Paris, 10-12 May 1995.

[13] A. Bouamrirène, *Coccinelle Results for PWER Rod Withdrawal Benchmark,* Specialists Meeting on LWR Core Transient Benchmarks NEA/NSC, Paris, 10-12 May 1995.

[14] D. Pevec, S. Langenbuch, K. Velkov, *Preliminary QUABOX/CUBBOX Results for Static Conditions,* Specialists Meeting on LWR Core Transient Benchmarks NEA/NSC, Paris, 10-12 May 1995.

[15] R. Fraikin, M. Mélice, *NEA-NSC PWR Benchmark Proposal*, NEA/NSC Specialists Meeting on LWR Core Transient Benchmarks, NEA/NSC, Paris (May 1995).

[16] E. Sartori, *NEA/NSC Specialists Meeting on Light Water Reactor Core Transient Benchmarks, Summary Report*," NEA/NSC/DOC(95)12 (May 1995).

[17] J.C. Kuijper, *Final PANTHER Solution to NEA-NSC 3-D PWR Core Transient Benchmark – Uncontrolled Withdrawal of Control Rods at Zero Power,* ECN-R-96-005 (May 1996).

[18] A.L. Casadei, *Reactor Physics in US Power Generation: Key Role in a Changing Industry*, Physor 1996, Mito, Japan, pp. O-1/8 (Sep. 1996).

[19] M. Mélice, C. Schneidesch, *OKAPI, A Code Coupling Spatial Kinetics to System Thermohydraulics for PWR Cores*, PHYSOR'96, Mito, Japan, pp. J-11/20 (Sep. 1996).

[20] U. Grundmann, U. Rohde, *DYN3D – a Three-Dimensional Core Model for Steady State and Transient Analysis in Thermal Reactors*, Physor 1996, Mito, Japan, pp. J-70/79 (Sep. 1996).

[21] R. Fraikin, *Review of a NEA-NSC PWR Benchmark on Uncontrolled Withdrawal of Control Rods at Zero Power*, Physor 1996, Mito, Japan, pp. J-99/108 (Sep. 1996).

[22] T. Lefvert, *OECD/NEA Ringhals 1 Stability Benchmark,* Physor 1996, Mito, Japan, pp. J-109/120 (Sep. 1996).

[23] T. Lefvert, *Ringhals 1 Stability Benchmark,* NEA/NSC/DOC(96)22 (Nov. 1996).

APPENDIX A

List of participants and contributors

BELGIUM	FRAIKIN R.	
	MAES Ph	
	MELICE M.	
	SCHNEIDESCH Ch.	Tractebel Energy Engineering
FRANCE	AIGLE R.	
	DAUDIN L.	
	GONNET M.	
	PETIARD M.	FRAMATOME
	BOUAMRIRENE A.	Electricité de France (EDF - DER)
	SARTORI E.	OECD/NEA
GERMANY	BAUER H.	
	FINNEMANN H.	Siemens AG, Power Generation Group (KWU)
	LANGENBUCH S.	Gesellschaft für Anlagen und Reaktorsicherheid
	VELKOV K.	(GRS)
ITALY	ALLOGGIO G.	
	BREGA E.	ENEL (ATN-GNUM)
KROATIA	GRGIC D.	
	PEVEC D.	University of Zagreb
NETHERLANDS	KUIJPER J.	Energieonderzoek Centrum Nederland (ECN)
REPUBLIC OF CHINA	HSIEH H-M.	Institute of Nuclear Energy Research (INER)
UNITED KINGDOM	BROHAN Ph.	
	HUTT P.	Nuclear Electric
USA	BORKOWSKI J.	
	ESSER P.	
	SMITH K.	Studsvik of America

APPENDIX B

Time histories plots

The following plots are given for Cases A, B and D; the results for Case C are very close to those obtained for Case B and have therefore been omitted here:

- fission power (C1);
- coolant heating (C2);
- coolant outlet temperature (C3);
- fuel Doppler temperature (C4);
- hot pellet fission power (D1);
- hot pellet coolant heating (D2);
- hot channel outlet temperature (D3);
- hot channel heat exchange coefficient (D4);
- hot pellet fuel enthalpy (D5);
- hot pellet centreline temperature (D6);
- hot pellet cladding outer surface temperature (D7).

Remarks

In some cases, the time steps used in the hot pellet output were different from those used for the core averaged results. We applied therefore an interpolation to homogenise the time abscissa.

KWU provided the hot pellet results with a time step of about 1 s; to avoid a non significant "triangular" evolution due to this interpolation, we removed the initial part of the evolution from some plots for Cases B and D.

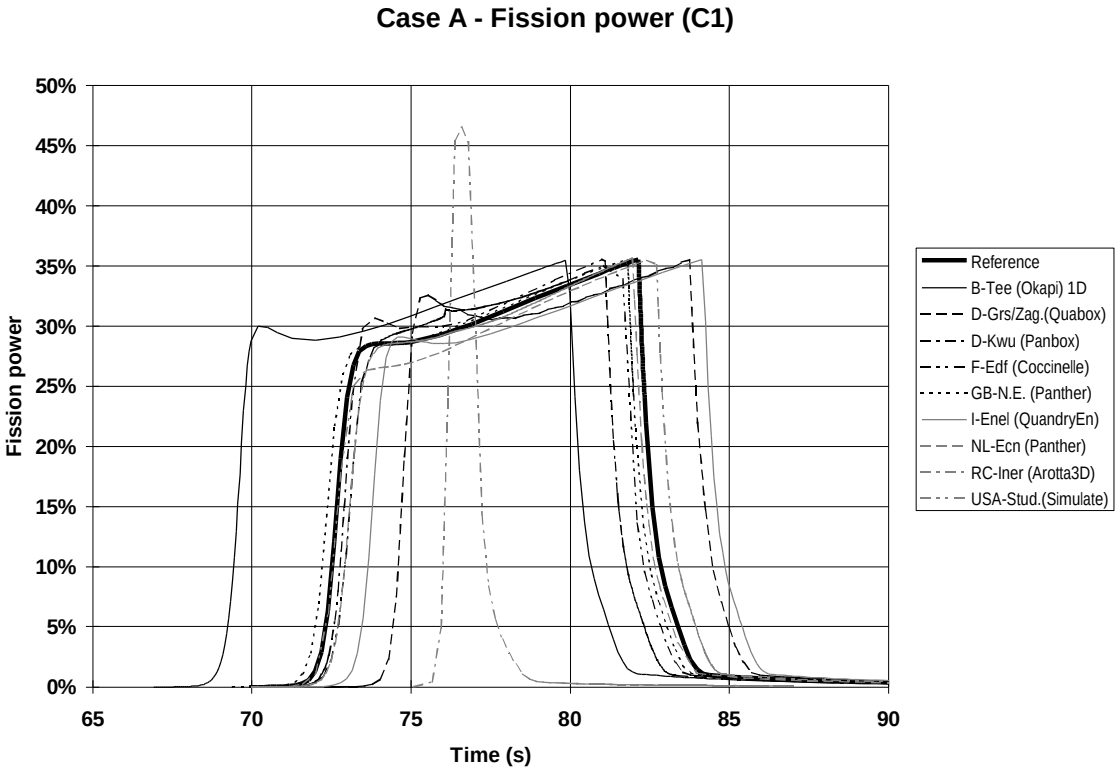
Case A - Fission power (C1)
Fission power
50%
45%
40%
35%
30%
25%
20%
15%
10%
5%
0%
65
70
75
80
85
90
Time (s)
Reference
B-Tee (Okapi) 1D
D-Grs/Zag.(Quabox)
D-Kwu (Panbox)
F-Edf (Coccinelle)
GB-N.E. (Panther)
I-Enel (QuandryEn)
NL-Ecn (Panther)
RC-Iner (Arotta3D)
USA-Stud.(Simulate)

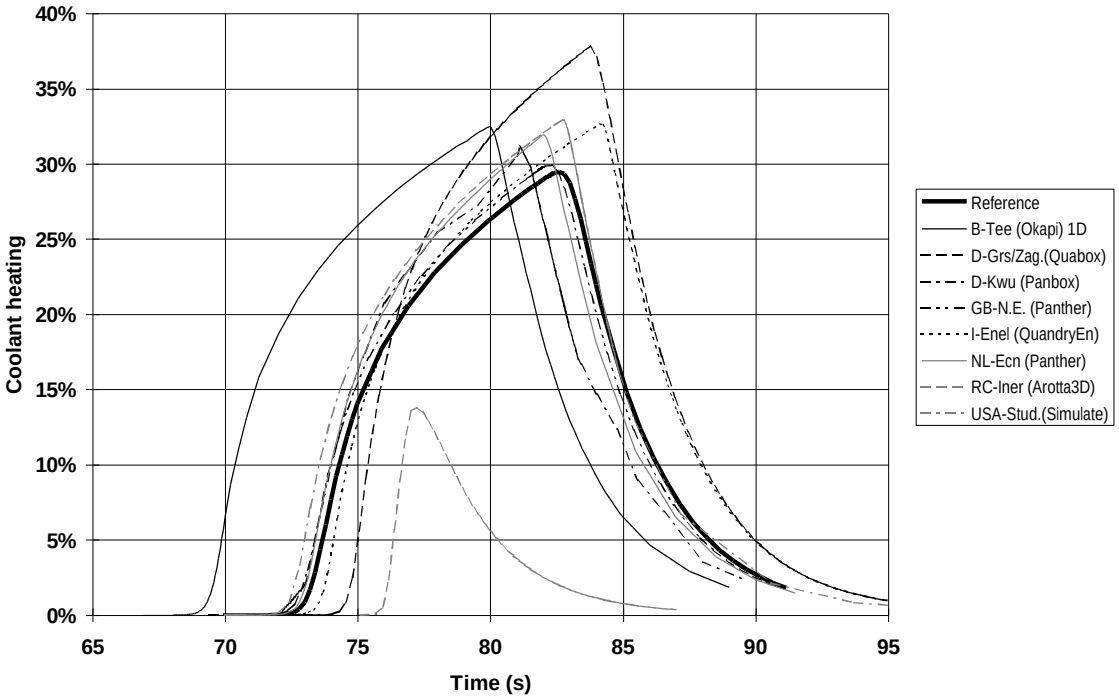
Case A - Coolant heating (C2)
Coolant heating
40%
35%
30%
25%
20%
15%
10%
5%
0%
65
70
75
80
85
90
95
Time (s)
Reference
B-Tee (Okapi) 1D
D-Grs/Zag.(Quabox)
D-Kwu (Panbox)
GB-N.E. (Panther)
I-Enel (QuandryEn)
NL-Ecn (Panther)
RC-Iner (Arotta3D)
USA-Stud.(Simulate)

Case A - Coolant outlet temperature (C3)

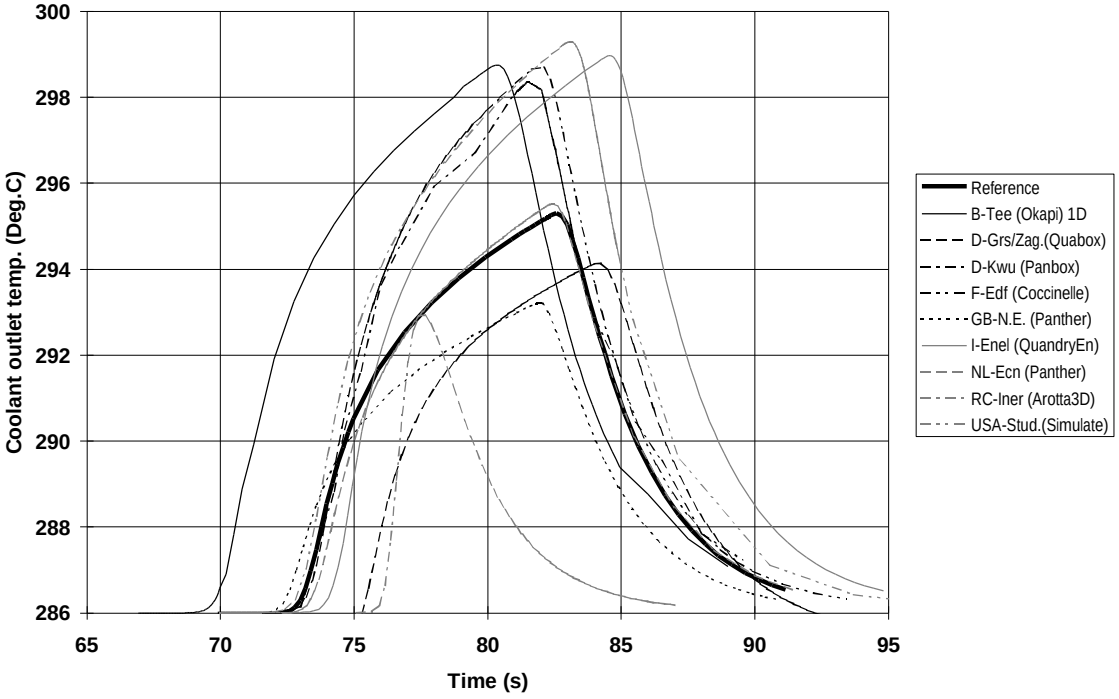

Case A - Fuel Doppler temperature (C4)

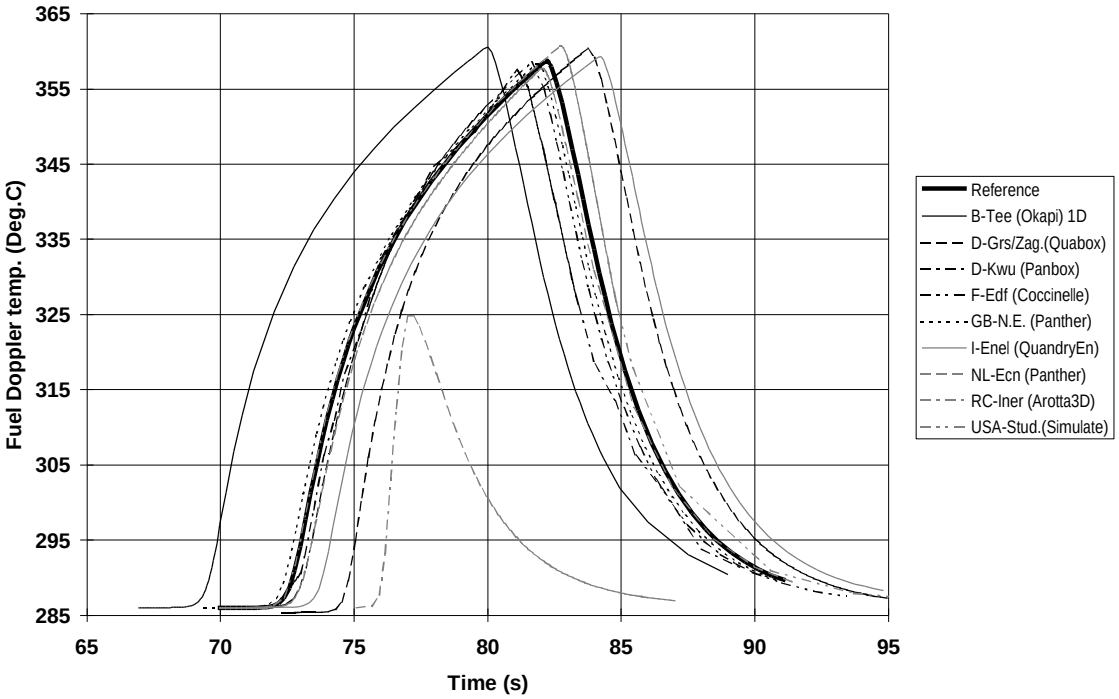

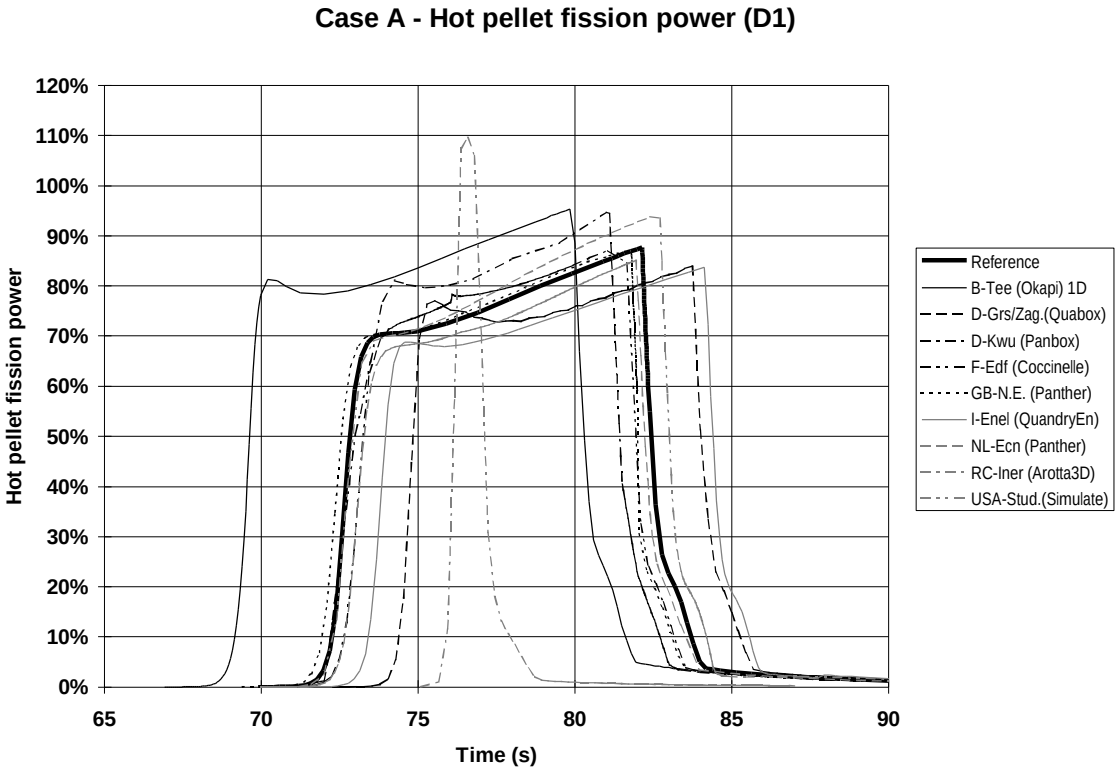
Case A - Hot pellet fission power (D1)
Hot pellet fission power
120%
110%
100%
90%
80%
70%
60%
50%
40%
30%
20%
10%
0%
65
70
75
80
85
90
Time (s)
Reference
B-Tee (Okapi) 1D
D-Grs/Zag.(Quabox)
D-Kwu (Panbox)
F-Edf (Coccinelle)
GB-N.E. (Panther)
I-Enel (QuandryEn)
NL-Ecn (Panther)
RC-Iner (Arotta3D)
USA-Stud.(Simulate)

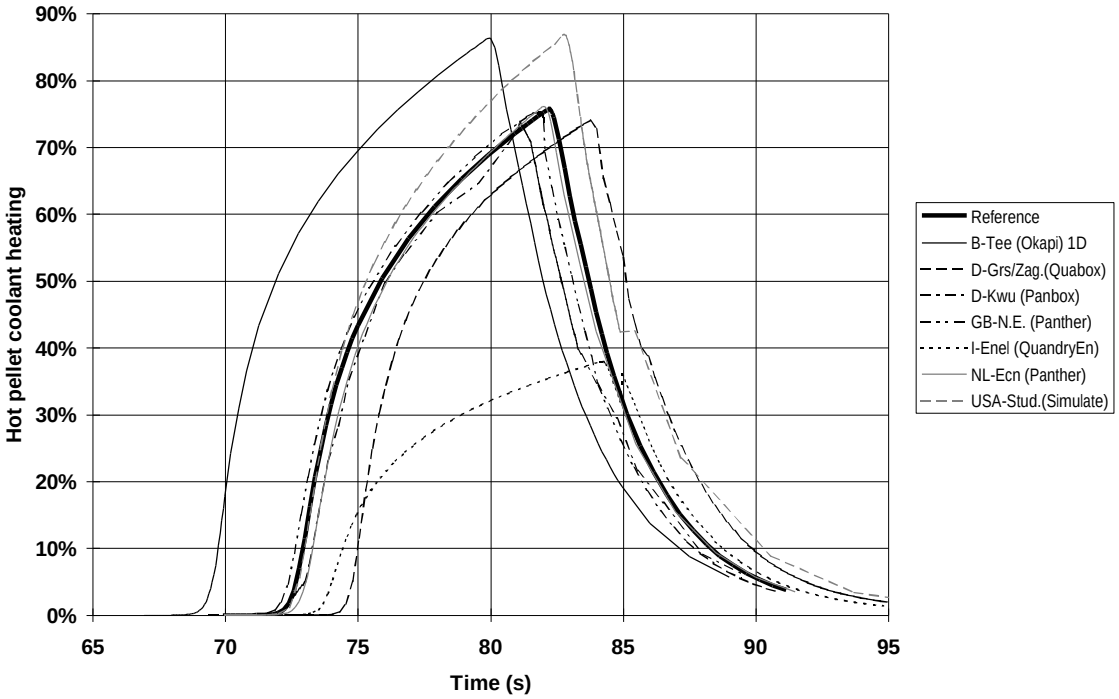
Case A - Hot pellet coolant heating (D2)
Hot pellet coolant heating
90%
80%
70%
60%
50%
40%
30%
20%
10%
0%
65
70
75
80
85
90
95
Time (s)
Reference
B-Tee (Okapi) 1D
D-Grs/Zag.(Quabox)
D-Kwu (Panbox)
GB-N.E. (Panther)
I-Enel (QuandryEn)
NL-Ecn (Panther)
USA-Stud.(Simulate)

Case A - Hot channel outlet temperature (D3)

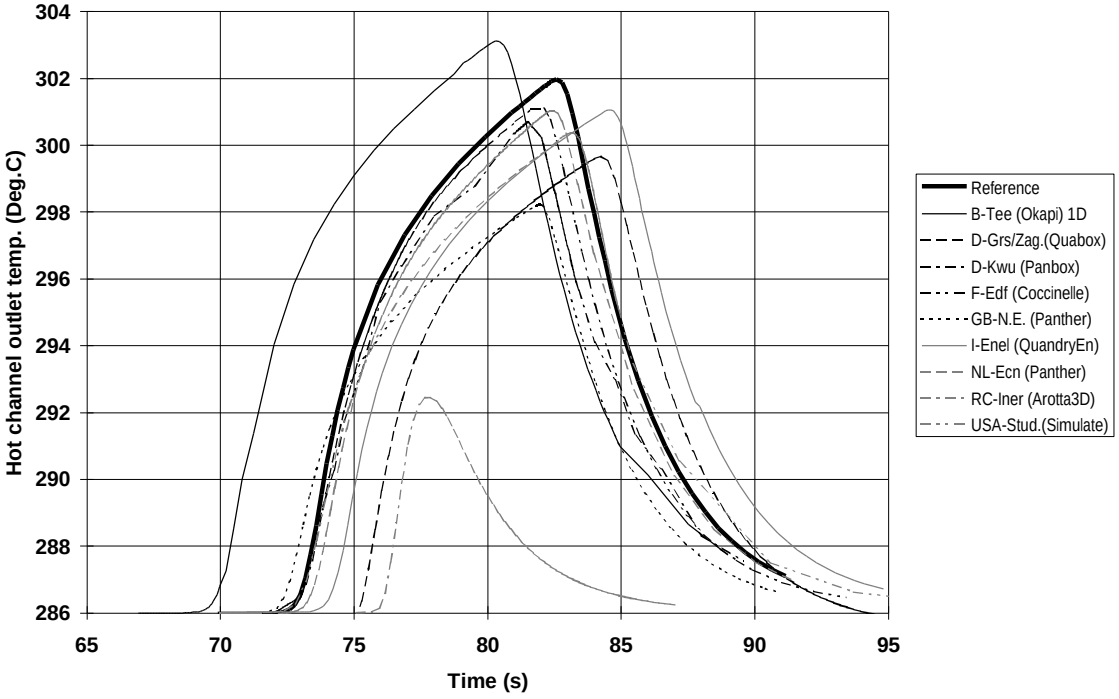

Case A - Hot channel heat exchange coefficient (D4)

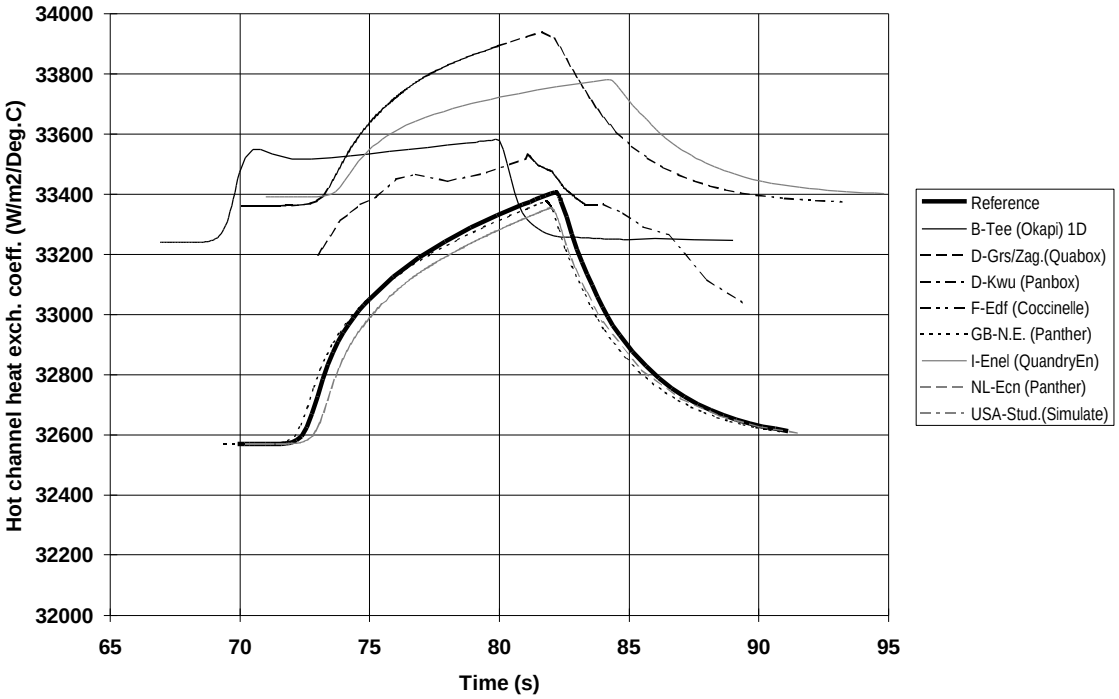

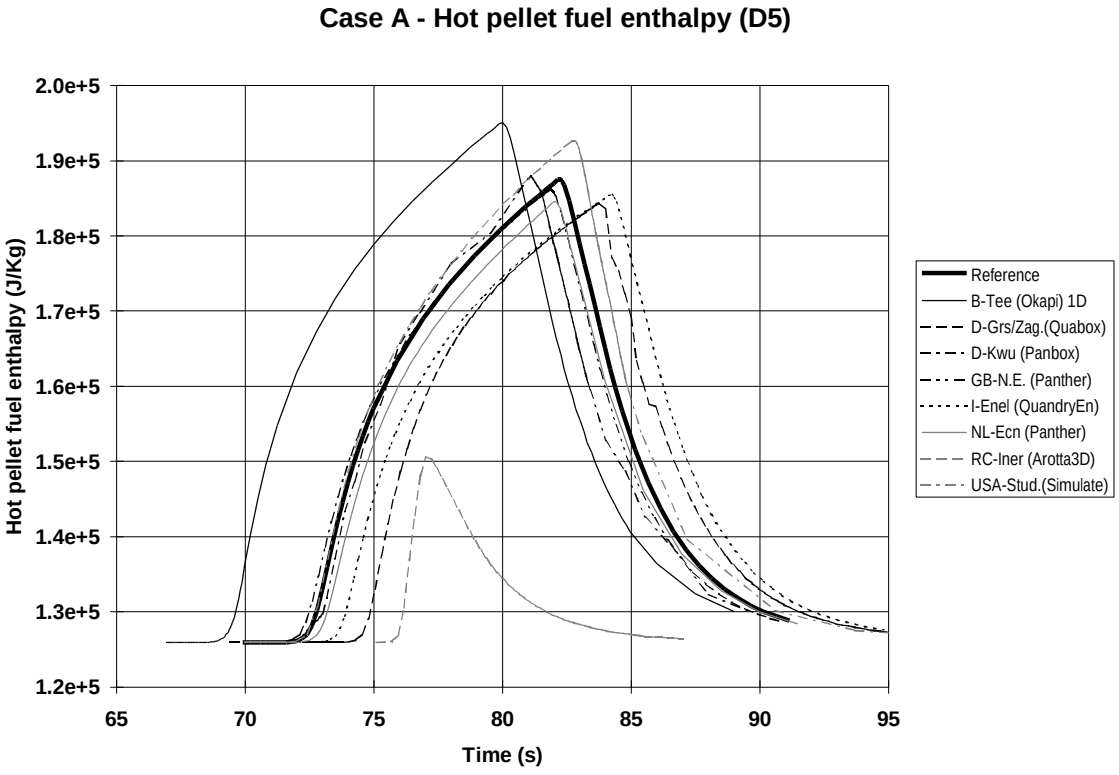
Case A - Hot pellet fuel enthalpy (D5)
Hot pellet fuel enthalpy (J/Kg)
2.0e+5
1.9e+5
1.8e+5
1.7e+5
1.6e+5
1.5e+5
1.4e+5
1.3e+5
1.2e+5
65
70
75
80
85
90
95
Time (s)
Reference
B-Tee (Okapi) 1D
D-Grs/Zag.(Quabox)
D-Kwu (Panbox)
GB-N.E. (Panther)
I-Enel (QuandryEn)
NL-Ecn (Panther)
RC-Iner (Arotta3D)
USA-Stud.(Simulate)

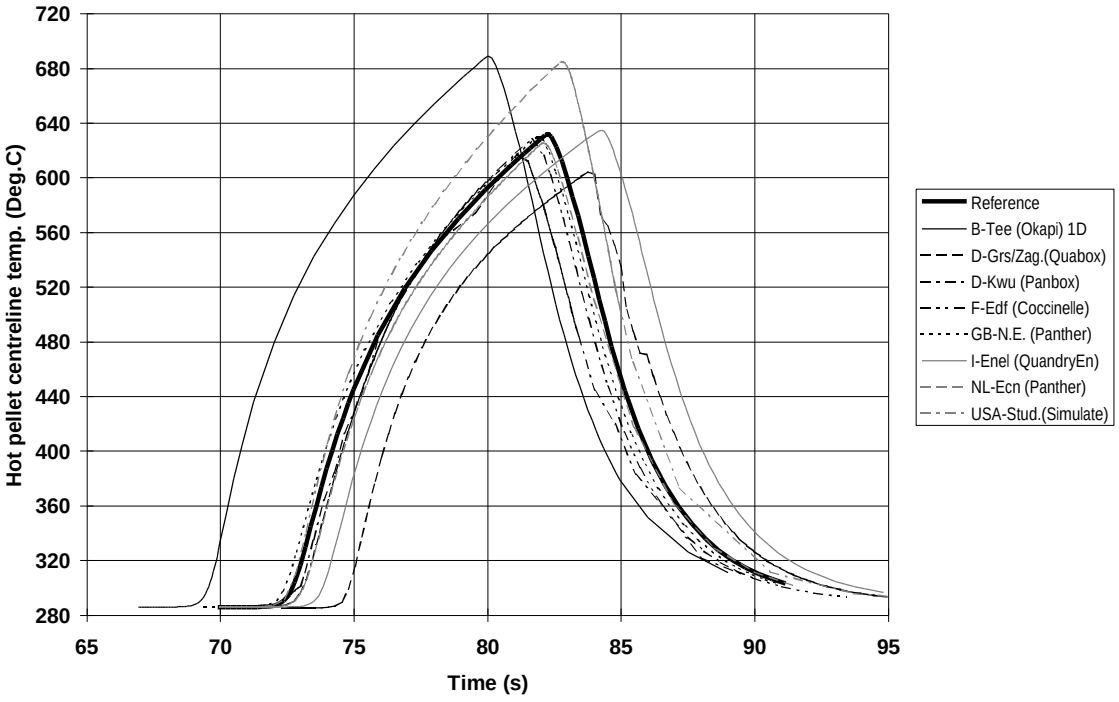
Case A - Hot pellet centreline temperature (D6)
Hot pellet centreline temp. (Deg.C)
720
680
640
600
560
520
480
440
400
360
320
280
65
70
75
80
85
90
95
Time (s)
Reference
B-Tee (Okapi) 1D
D-Grs/Zag.(Quabox)
D-Kwu (Panbox)
F-Edf (Coccinelle)
GB-N.E. (Panther)
I-Enel (QuandryEn)
NL-Ecn (Panther)
USA-Stud.(Simulate)

Case A - Hot pellet cladding outer surface temperature (D7)

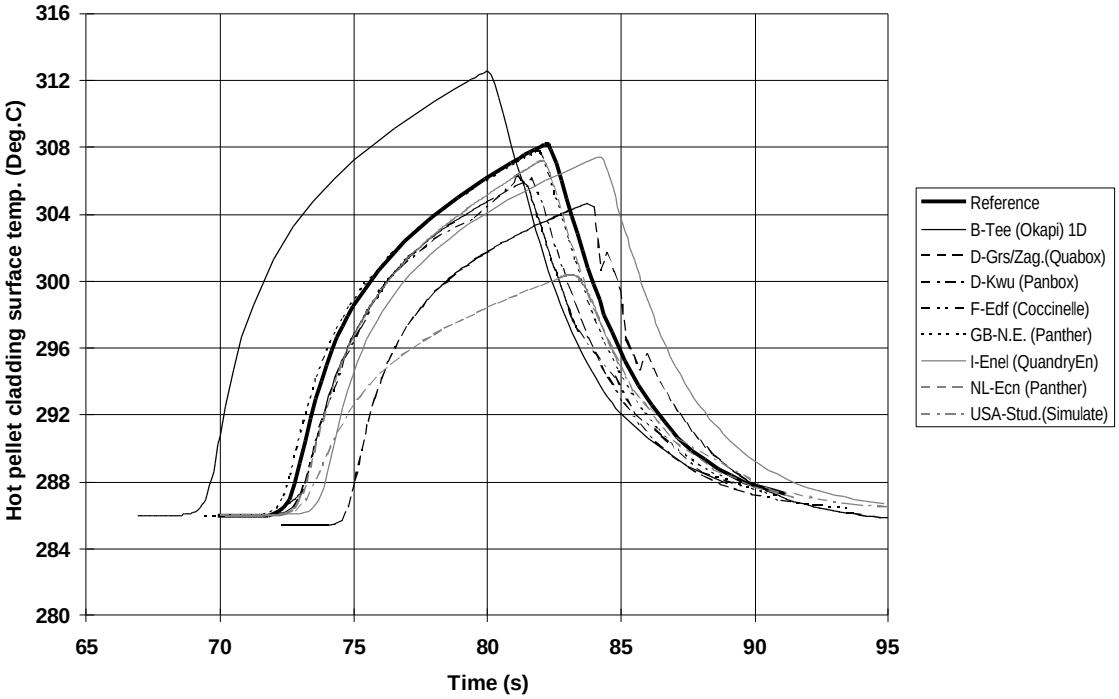

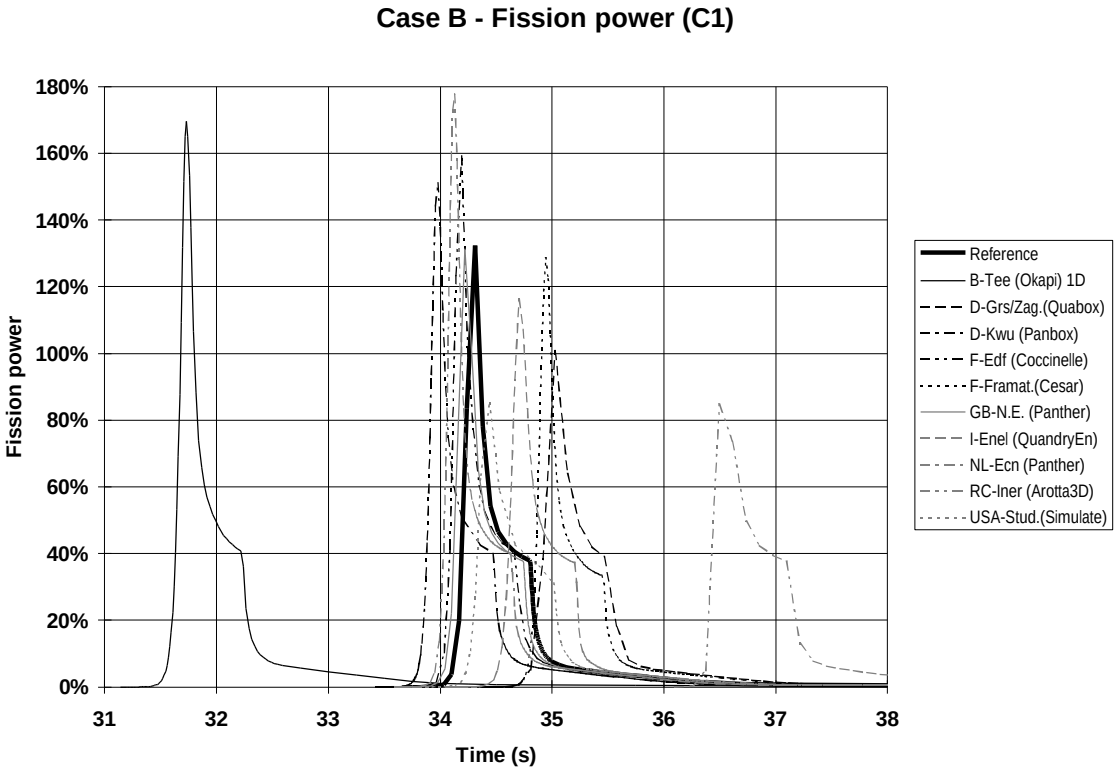
Case B - Fission power (C1)
Fission power
180%
160%
140%
120%
100%
80%
60%
40%
20%
0%
31
32
33
34
35
36
37
38
Time (s)
Reference
B-Tee (Okapi) 1D
D-Grs/Zag.(Quabox)
D-Kwu (Panbox)
F-Edf (Coccinelle)
F-Framat.(Cesar)
GB-N.E. (Panther)
I-Enel (QuandryEn)
NL-Ecn (Panther)
RC-Iner (Arotta3D)
USA-Stud.(Simulate)

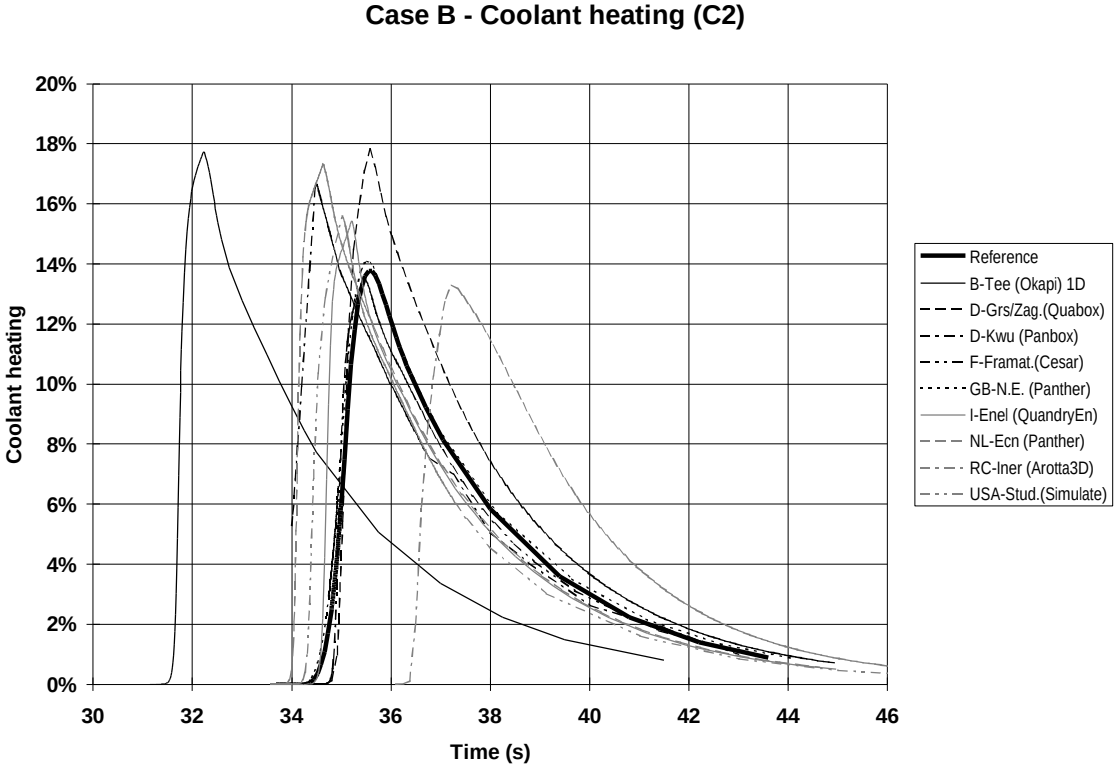
Case B - Coolant heating (C2)
Coolant heating
20%
18%
16%
14%
12%
10%
8%
6%
4%
2%
0%
30
32
34
36
38
40
42
44
46
Time (s)
Reference
B-Tee (Okapi) 1D
D-Grs/Zag.(Quabox)
D-Kwu (Panbox)
F-Framat.(Cesar)
GB-N.E. (Panther)
I-Enel (QuandryEn)
NL-Ecn (Panther)
RC-Iner (Arotta3D)
USA-Stud.(Simulate)

Case B - Coolant outlet temperature (C3)

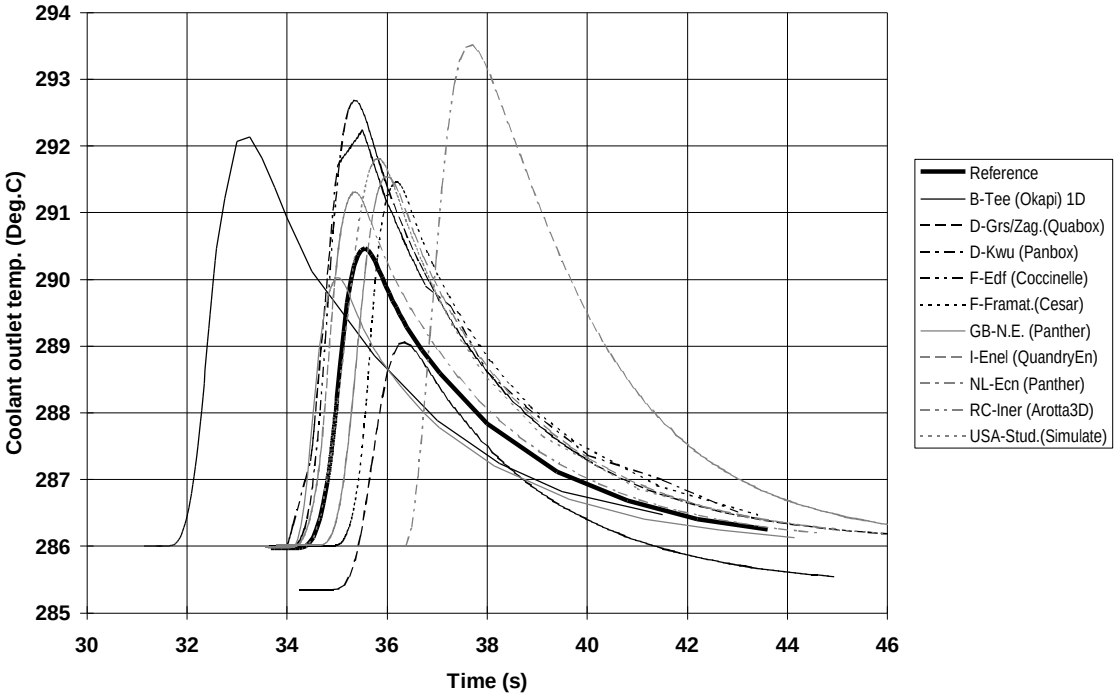

Case B - Fuel Doppler temperature (C4)

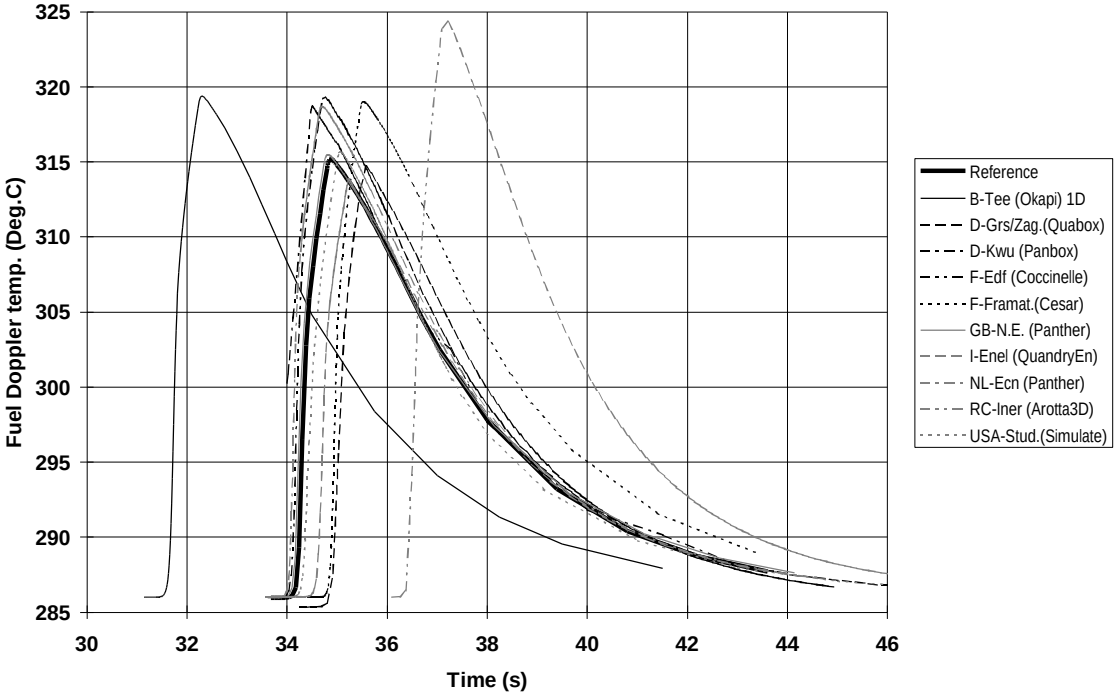

Case B - Hot pellet fission power (D1)

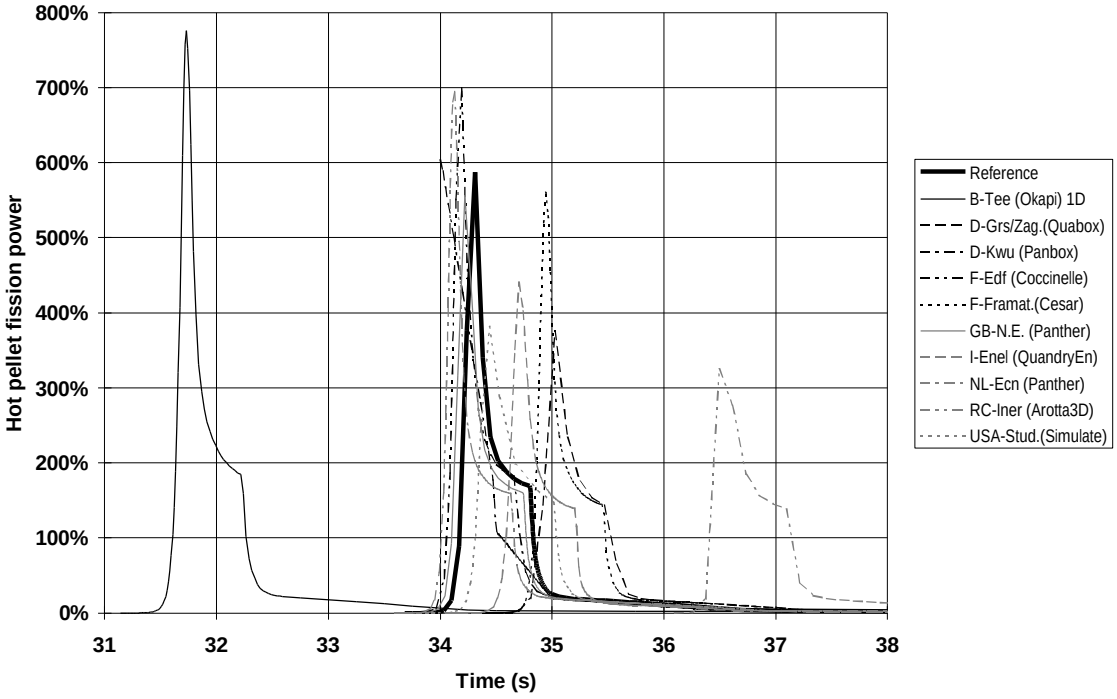

Case B - Hot pellet coolant heating (D2)

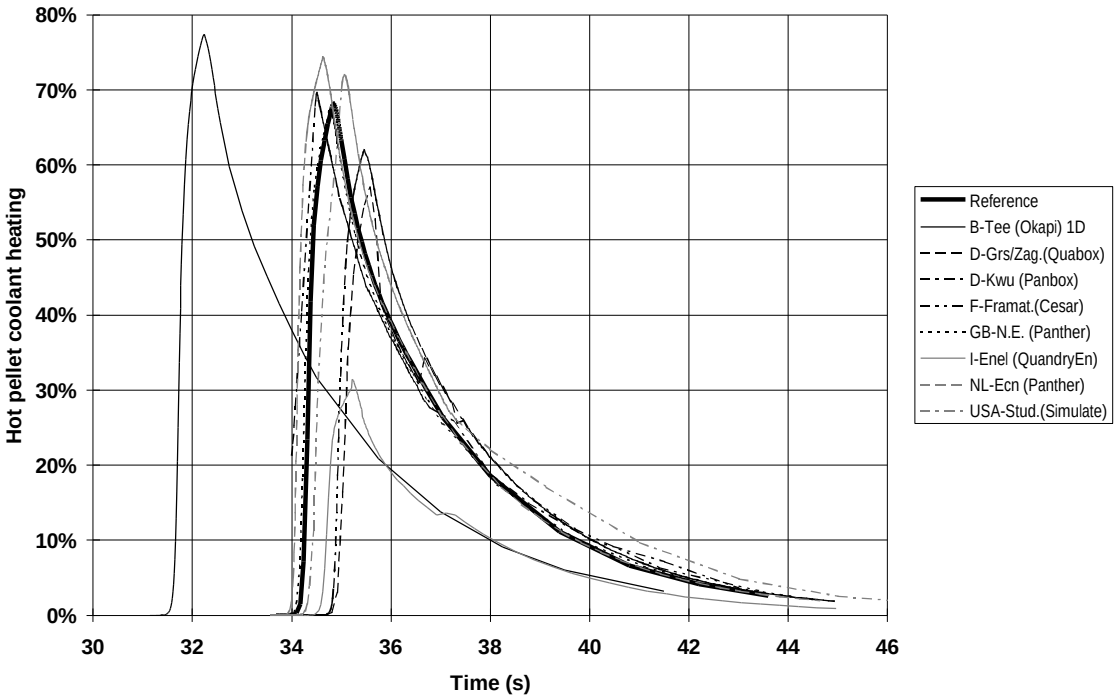

Case B - Hot channel outlet temperature (D3)

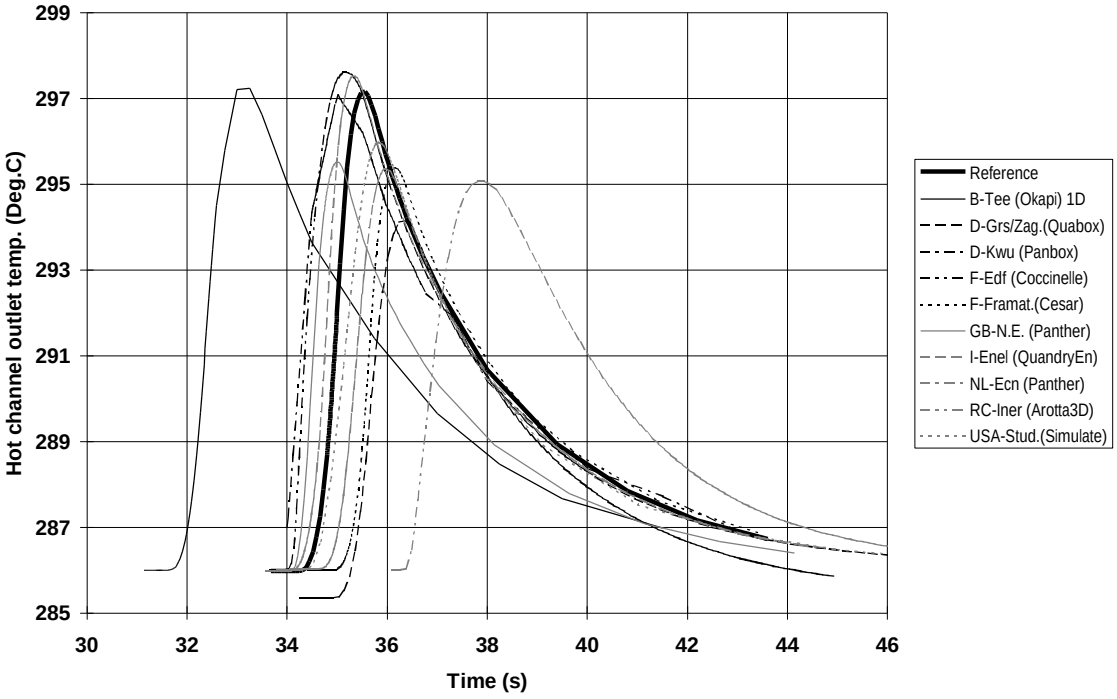

Case B - Hot channel heat exchange coefficient (D4)

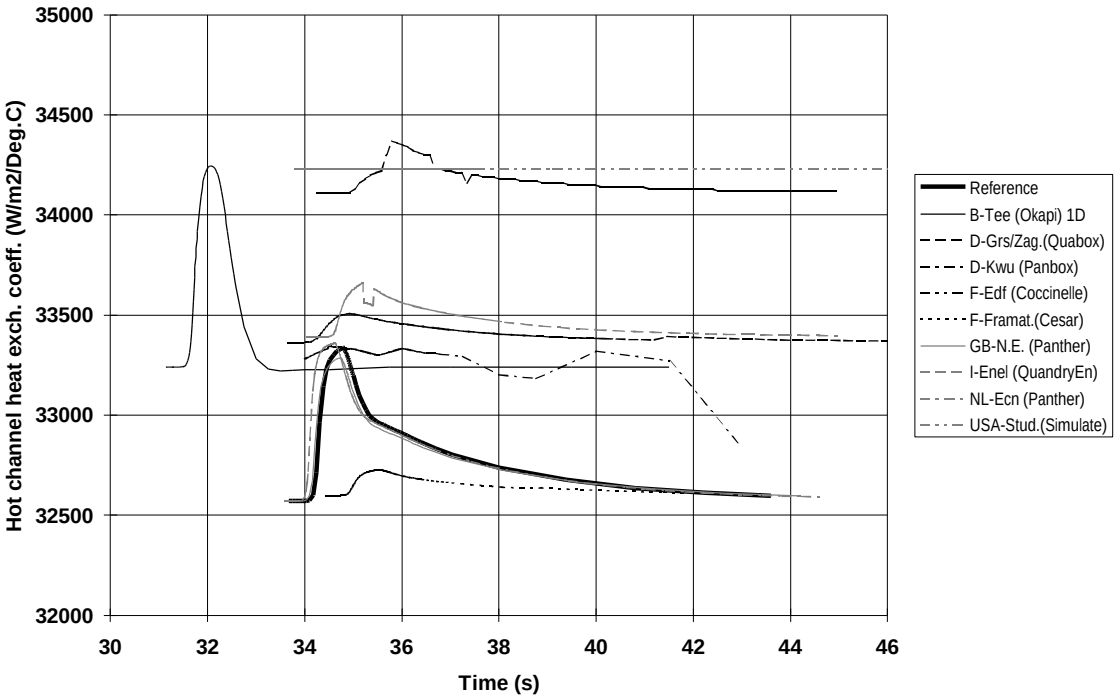

Case B - Hot pellet fuel enthalpy (D5)

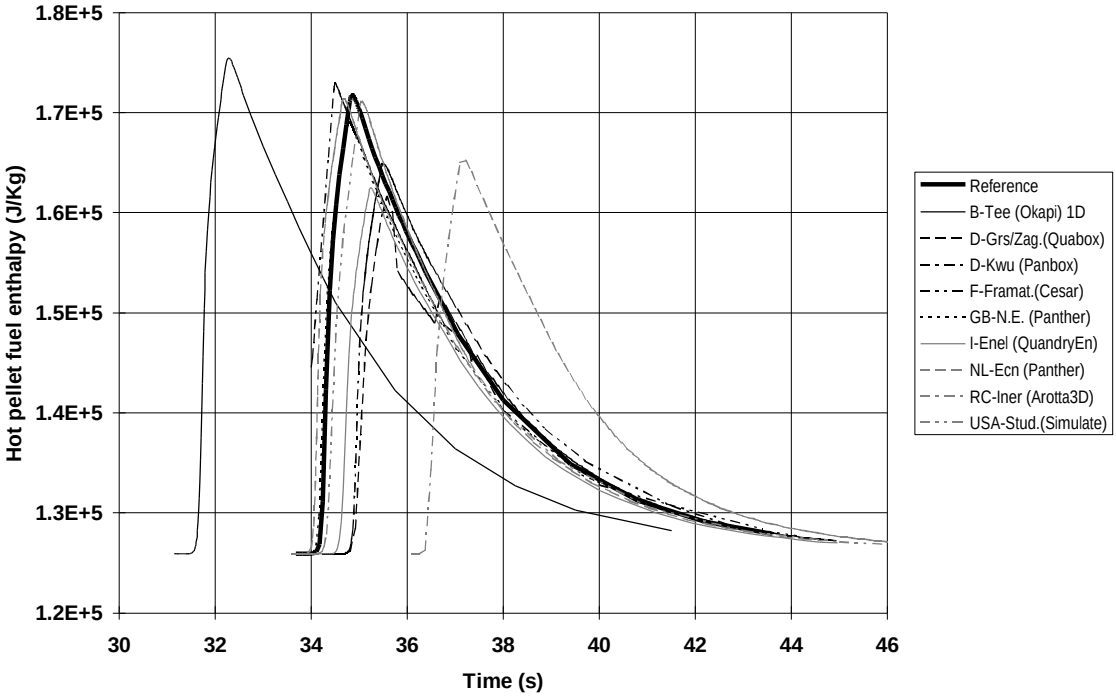

Case B - Hot pellet centreline temperature (D6)

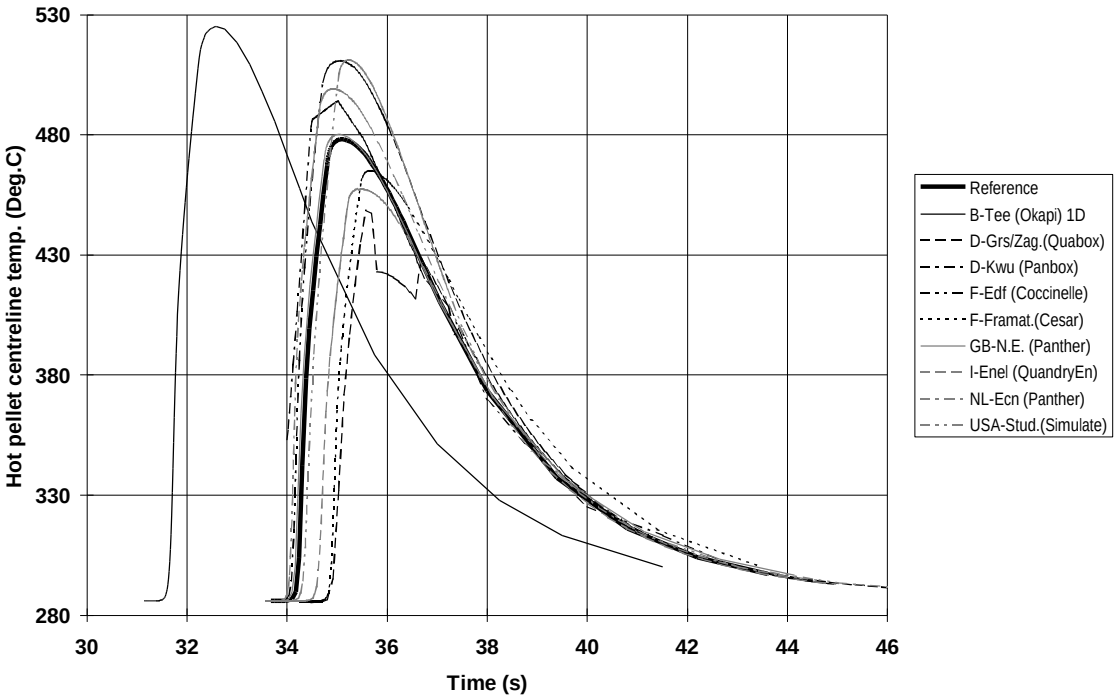

Case B - Hot pellet cladding outer surface temperature (D7)

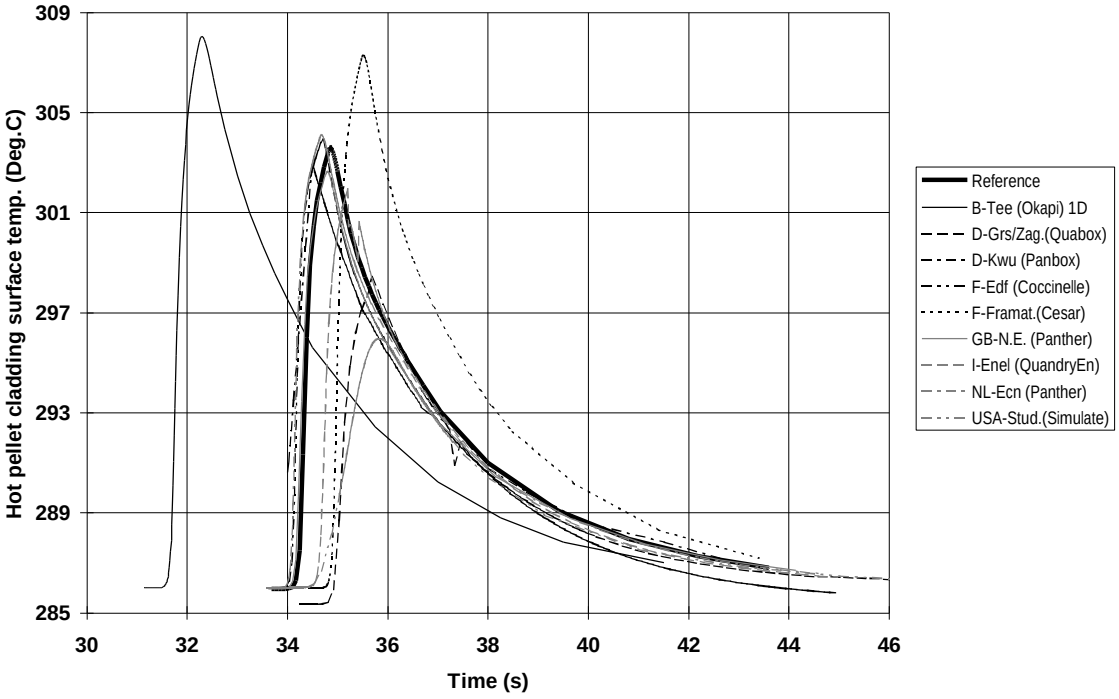

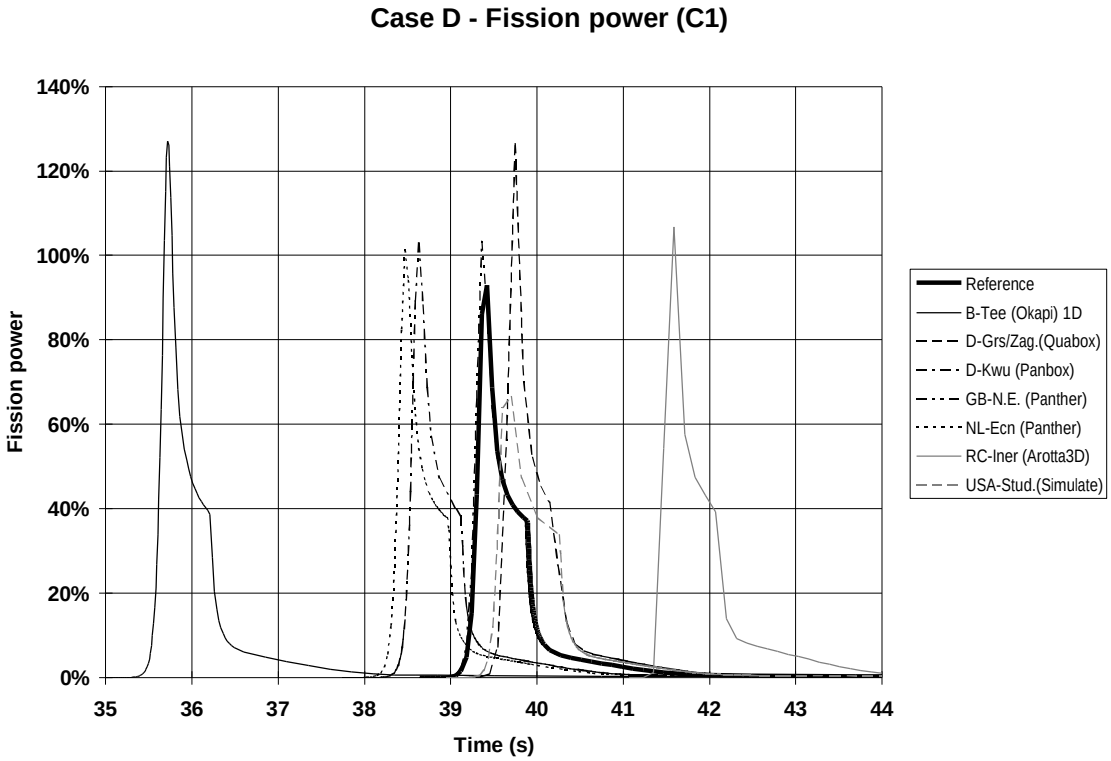
Case D - Fission power (C1)
Fission power
140%
120%
100%
80%
60%
40%
20%
0%
35
36
37
38
39
40
41
42
43
44
Time (s)
Reference
B-Tee (Okapi) 1D
D-Grs/Zag.(Quabox)
D-Kwu (Panbox)
GB-N.E. (Panther)
NL-Ecn (Panther)
RC-Iner (Arotta3D)
USA-Stud.(Simulate)

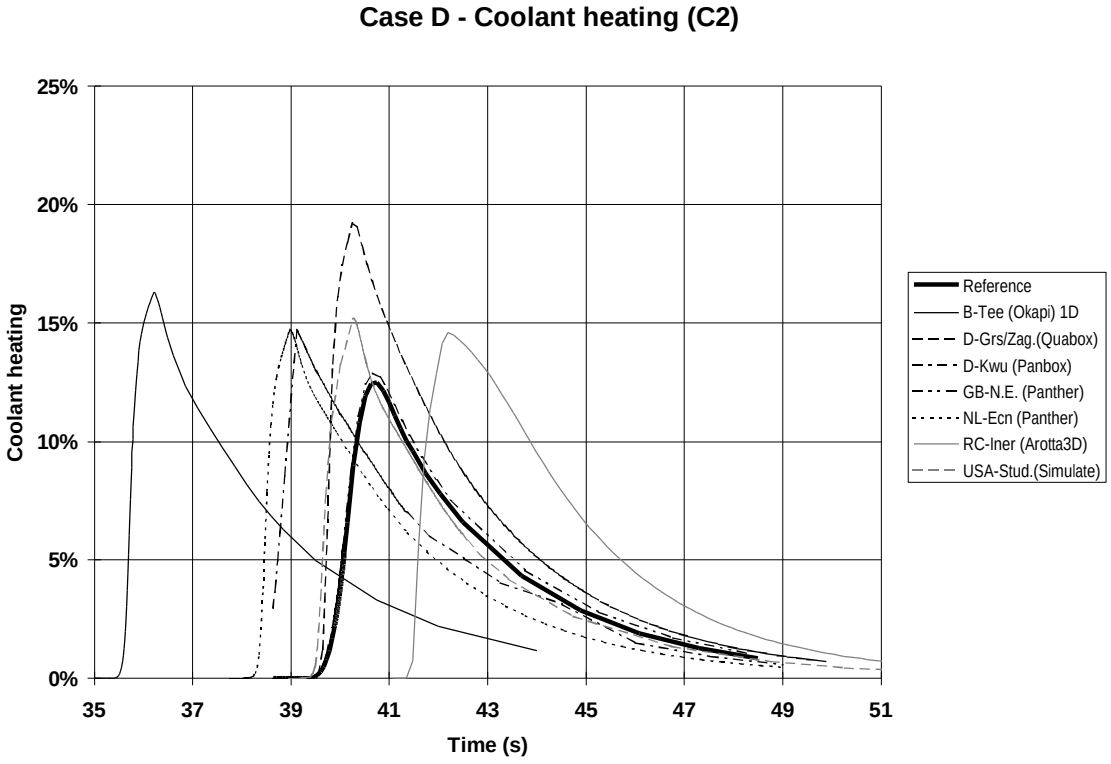
Case D - Coolant heating (C2)
Coolant heating
25%
20%
15%
10%
5%
0%
35
37
39
41
43
45
47
49
51
Time (s)
Reference
B-Tee (Okapi) 1D
D-Grs/Zag.(Quabox)
D-Kwu (Panbox)
GB-N.E. (Panther)
NL-Ecn (Panther)
RC-Iner (Arotta3D)
USA-Stud.(Simulate)

Case D - Coolant outlet temperature (C3)

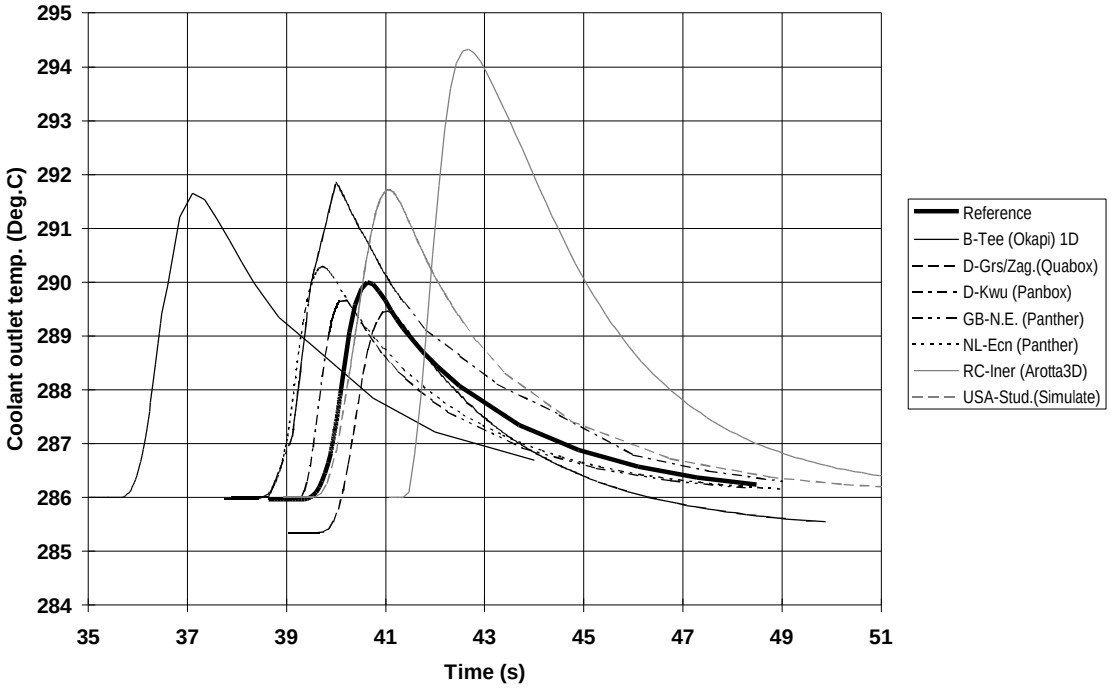

Case D - Fuel Doppler temperature (C4)

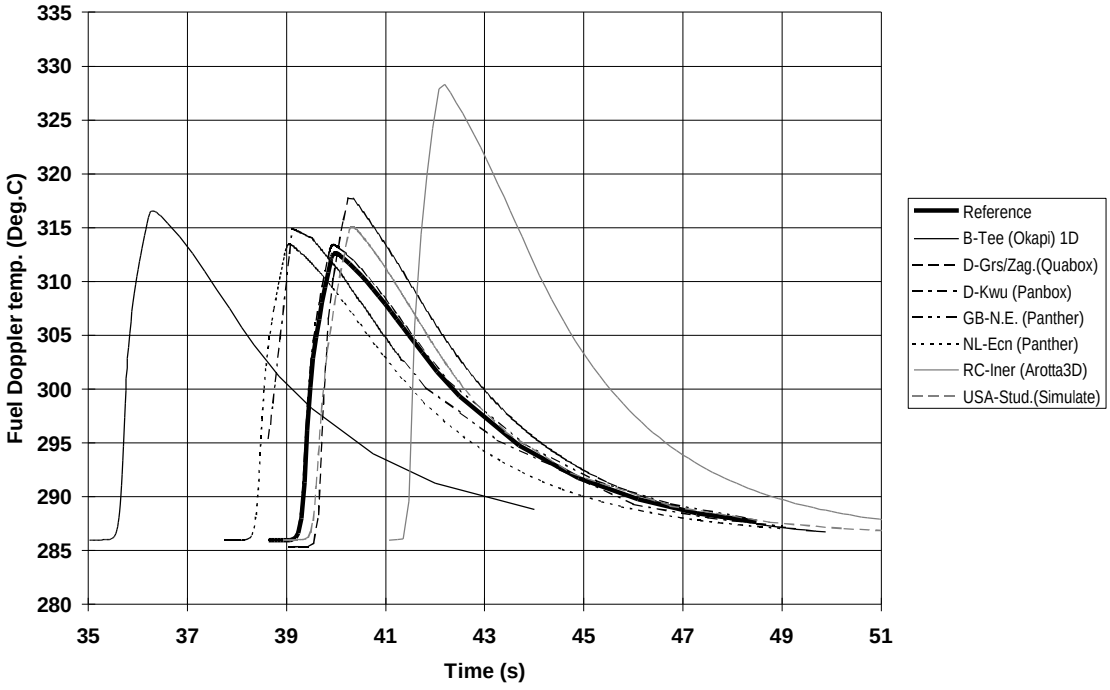

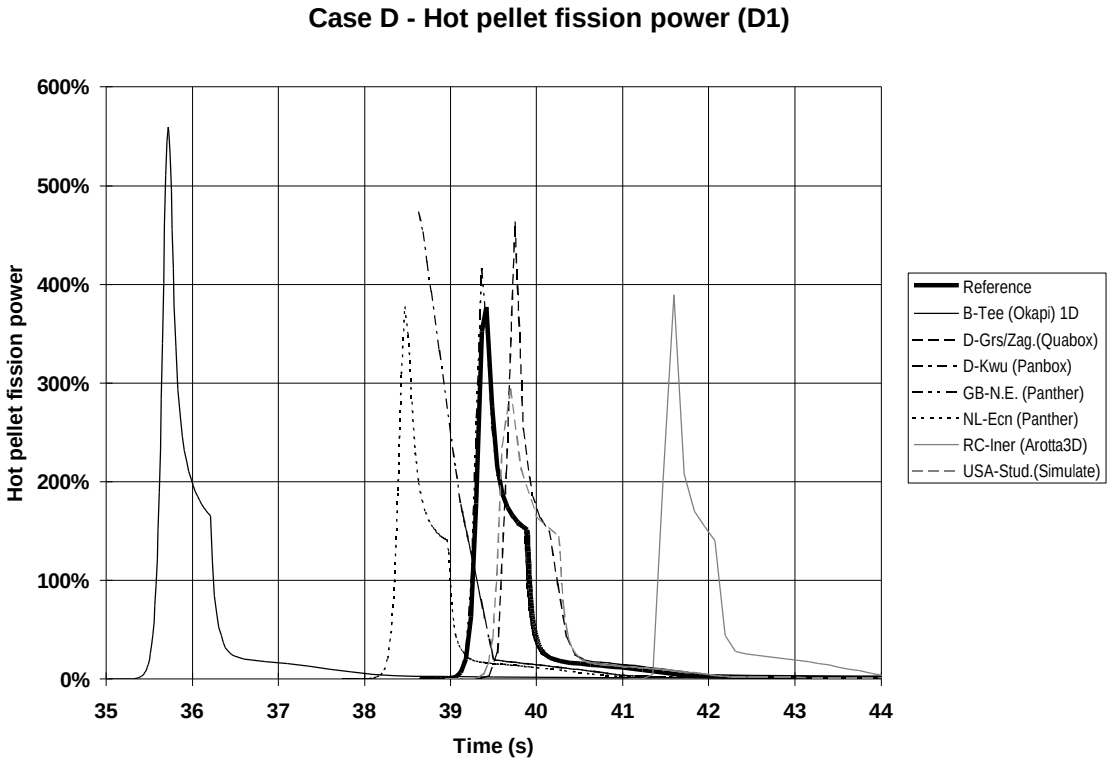
Case D - Hot pellet fission power (D1)
Hot pellet fission power
600%
500%
400%
300%
200%
100%
0%
35
36
37
38
39
40
41
42
43
44
Time (s)
Reference
B-Tee (Okapi) 1D
D-Grs/Zag.(Quabox)
D-Kwu (Panbox)
GB-N.E. (Panther)
NL-Ecn (Panther)
RC-Iner (Arotta3D)
USA-Stud.(Simulate)

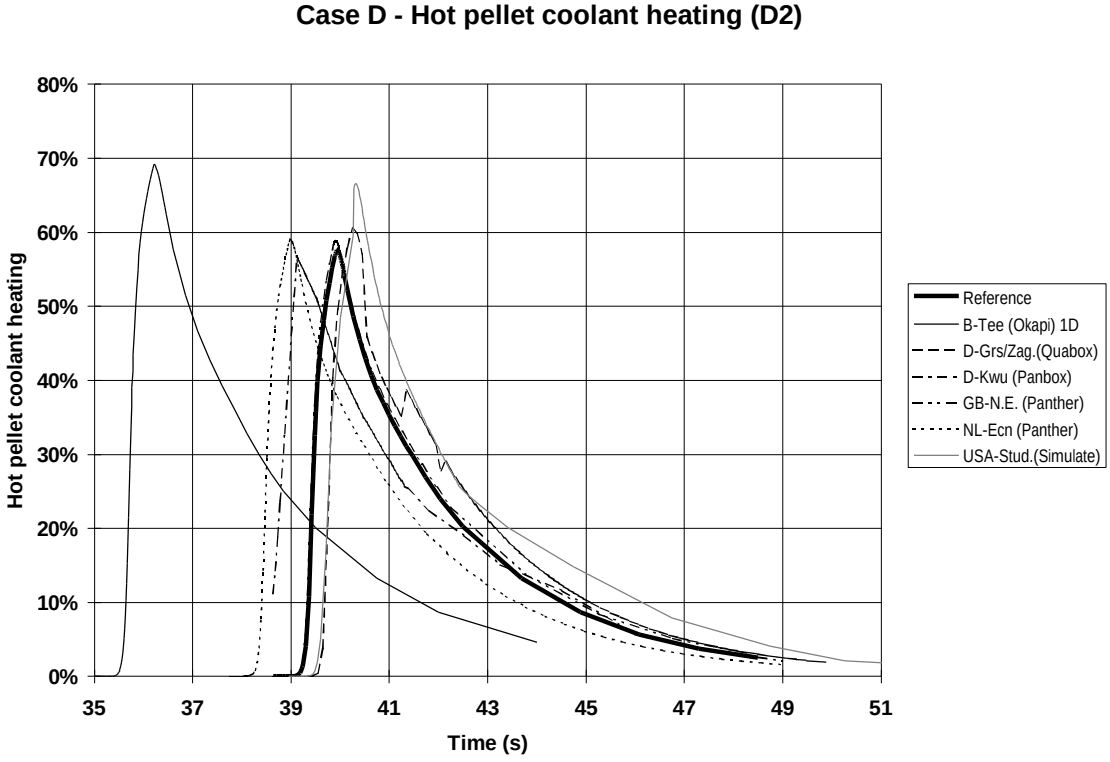
Case D - Hot pellet coolant heating (D2)
Hot pellet coolant heating
80%
70%
60%
50%
40%
30%
20%
10%
0%
35
37
39
41
43
45
47
49
51
Time (s)
Reference
B-Tee (Okapi) 1D
D-Grs/Zag.(Quabox)
D-Kwu (Panbox)
GB-N.E. (Panther)
NL-Ecn (Panther)
USA-Stud.(Simulate)

Case D - Hot channel outlet temperature (D3)

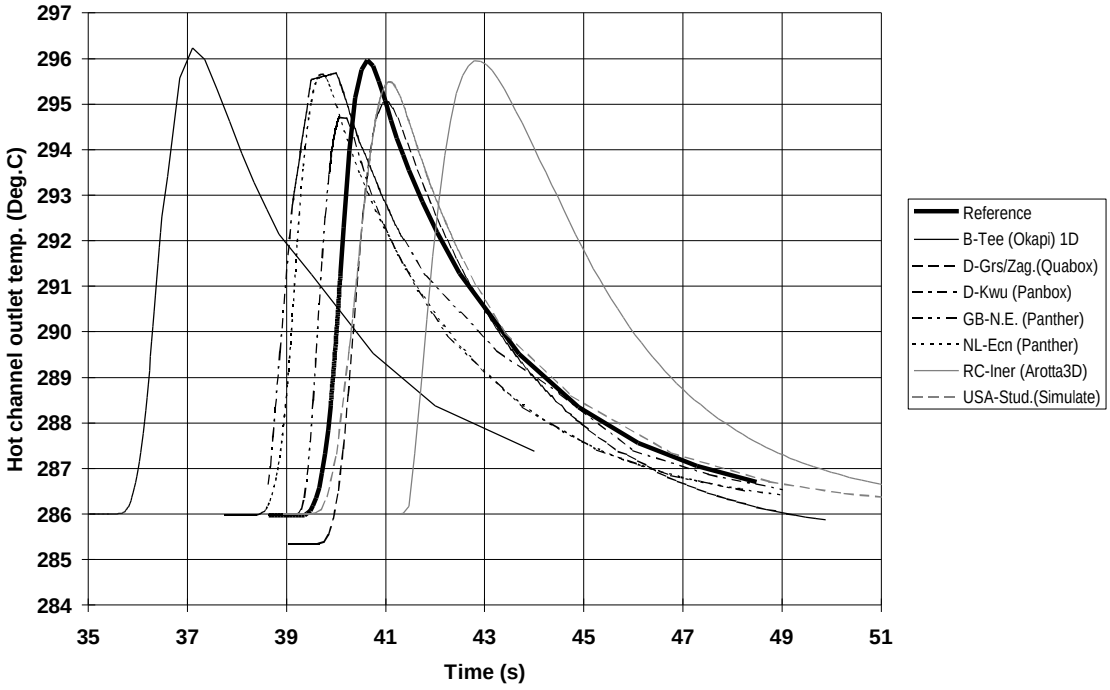

Case D - Hot channel heat exchange coefficient (D4)

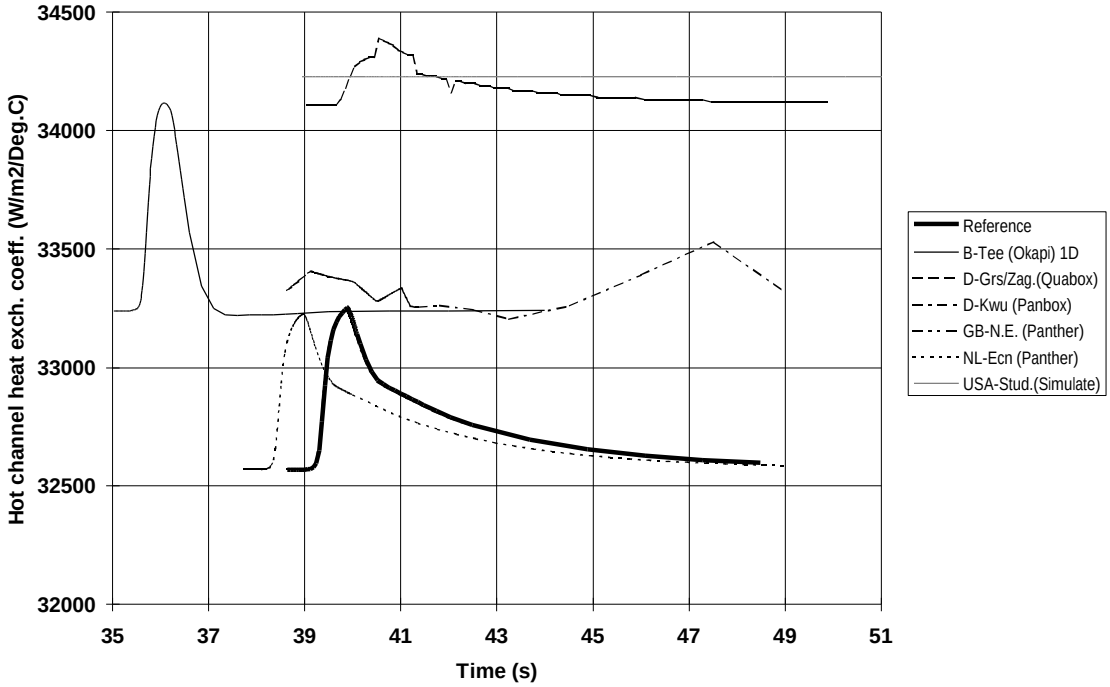

Case D - Hot pellet fuel enthalpy (D5)

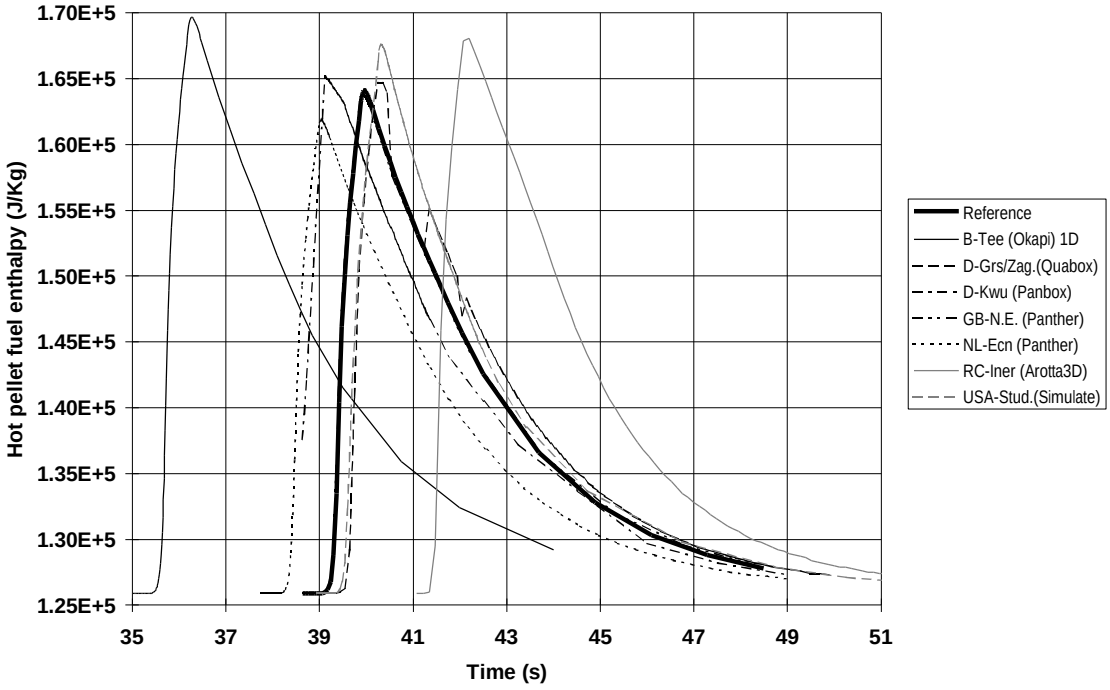

Case D - Hot pellet centreline temperature (D6)

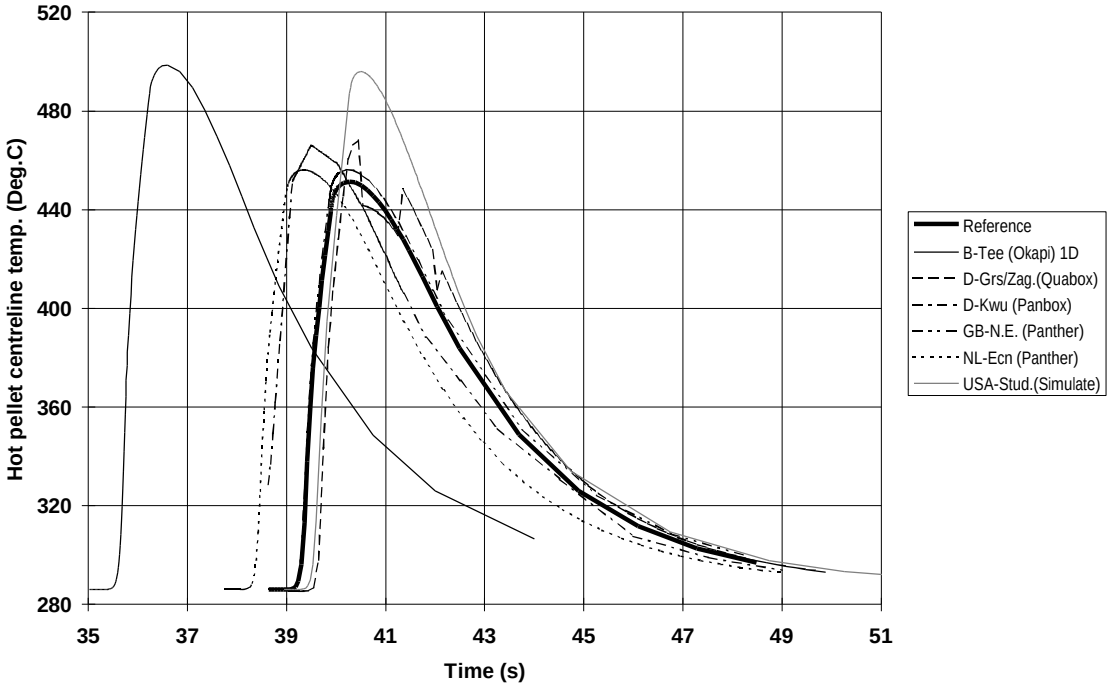

Case D - Hot pellet cladding outer surface temperature (D7)

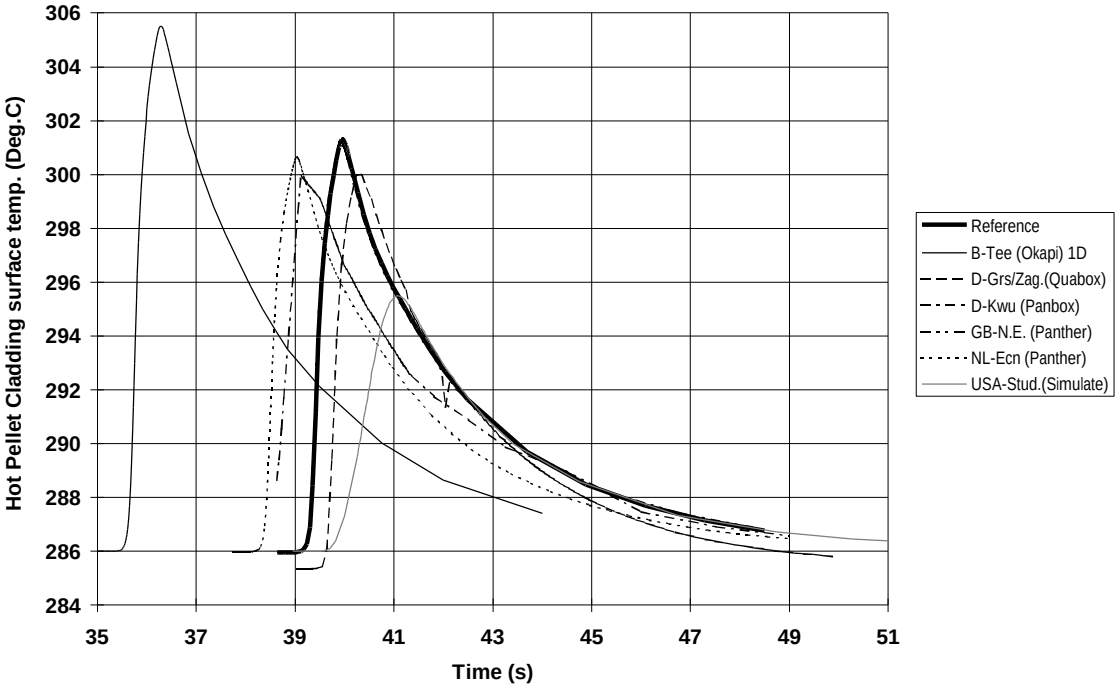

APPENDIX C

Axial power profiles

The following plots are given for Cases A, B and D; the results for Case C are very close to those obtained for Case B and have therefore been omitted here:

- axial power profile at initial steady state (B2);
- envelope axial power profile at initial steady state (B6);
- axial power profile at time of maximum power (E2);
- envelope axial power profile at time of maximum power (E6).

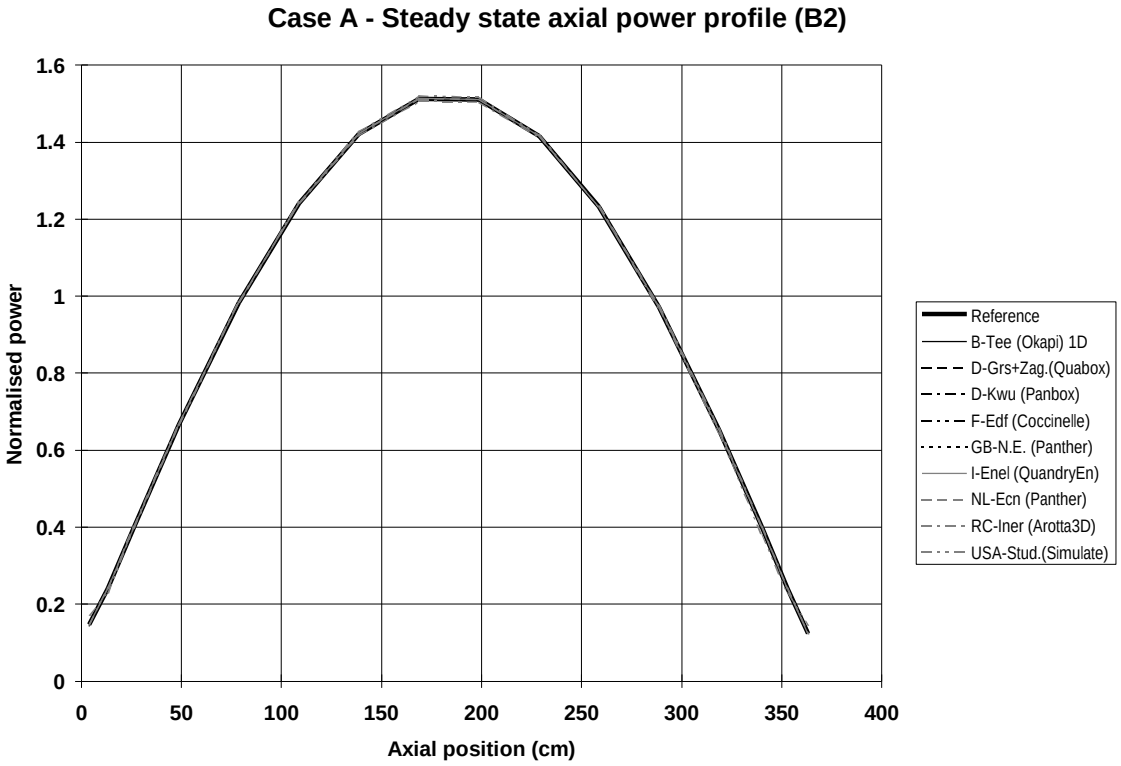
Case A - Steady state axial power profile (B2)
Normalised power
Axial position (cm)
0
0.2
0.4
0.6
0.8
1
1.2
1.4
1.6
0
50
100
150
200
250
300
350
400
Reference
B-Tee (Okapi) 1D
D-Grs+Zag.(Quabox)
D-Kwu (Panbox)
F-Edf (Coccinelle)
GB-N.E. (Panther)
I-Enel (QuandryEn)
NL-Ecn (Panther)
RC-Iner (Arotta3D)
USA-Stud.(Simulate)

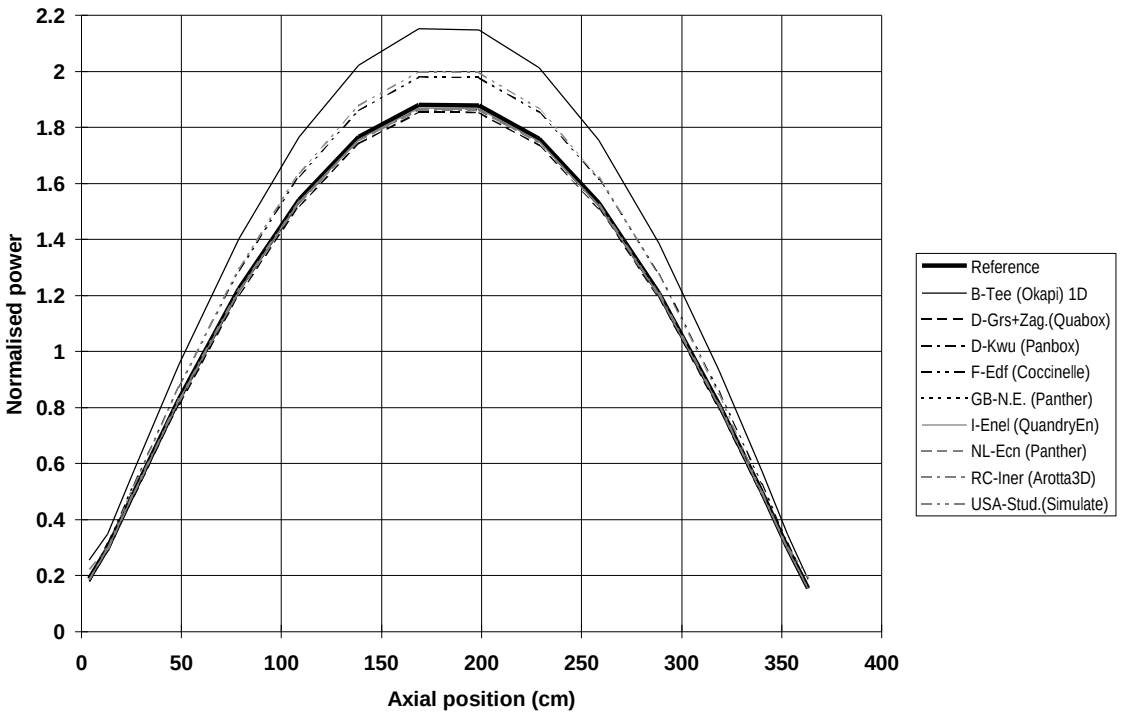
Case A - Steady state envelope axial power profile (B6)
Normalised power
Axial position (cm)
0
0.2
0.4
0.6
0.8
1
1.2
1.4
1.6
1.8
2
2.2
0
50
100
150
200
250
300
350
400
Reference
B-Tee (Okapi) 1D
D-Grs+Zag.(Quabox)
D-Kwu (Panbox)
F-Edf (Coccinelle)
GB-N.E. (Panther)
I-Enel (QuandryEn)
NL-Ecn (Panther)
RC-Iner (Arotta3D)
USA-Stud.(Simulate)

Case A - Axial power profile at T.max (E2)

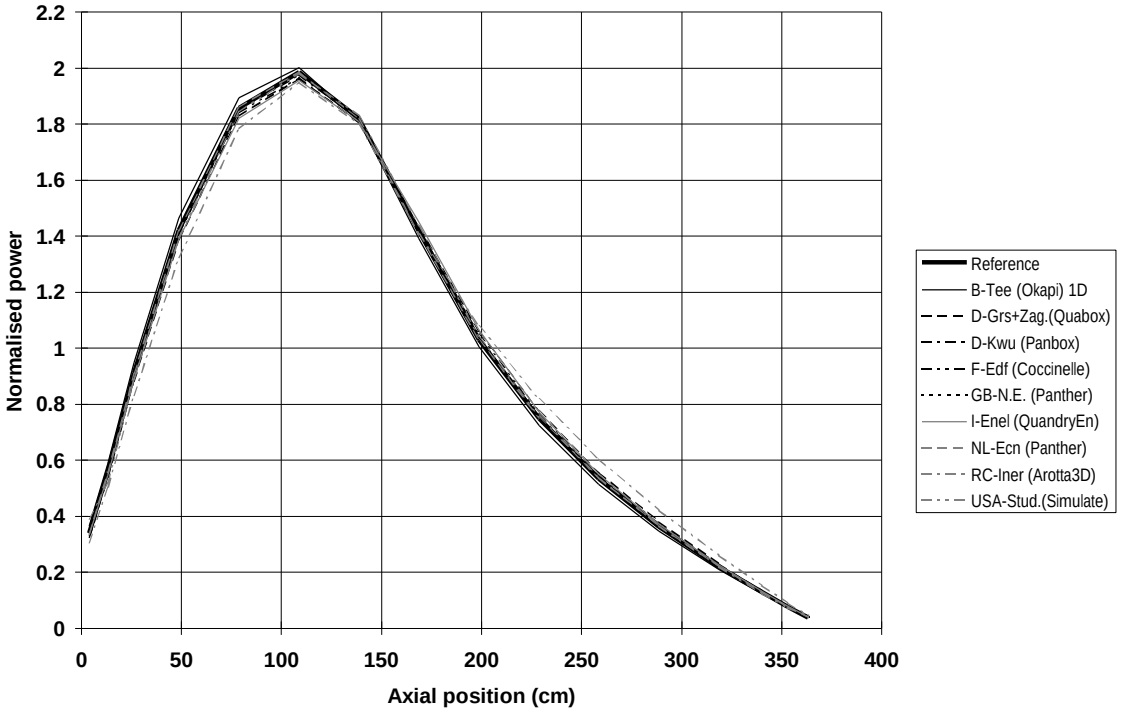

Case A - Envelope axial power profile at T.max (E6)

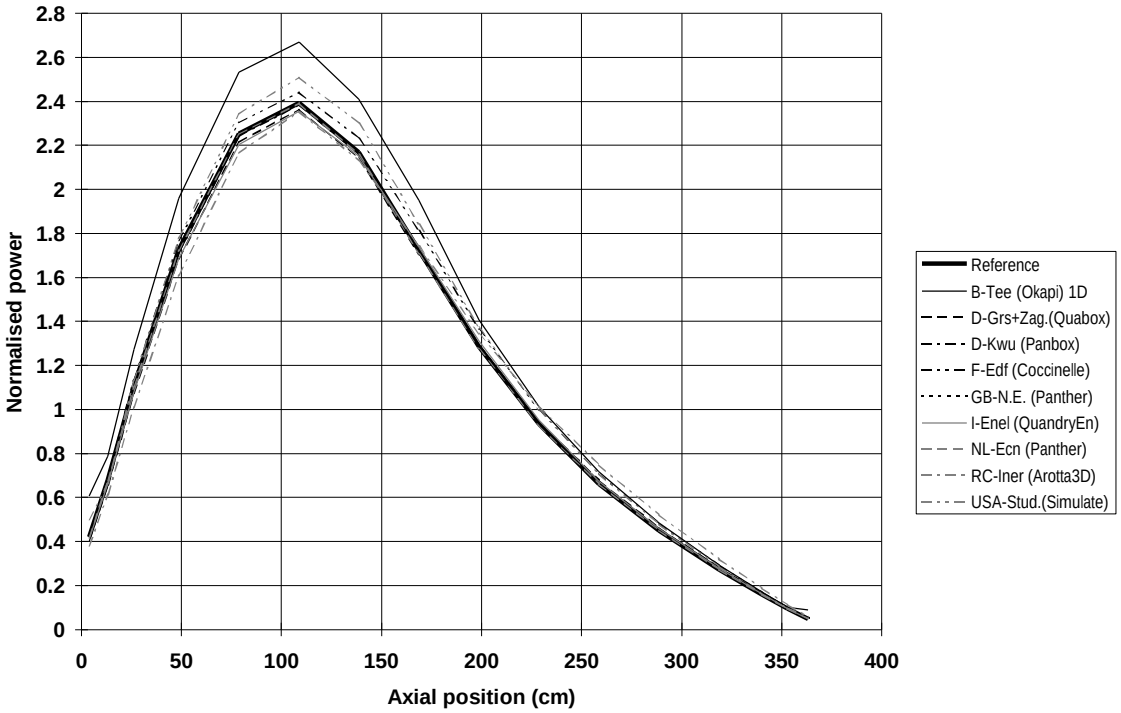

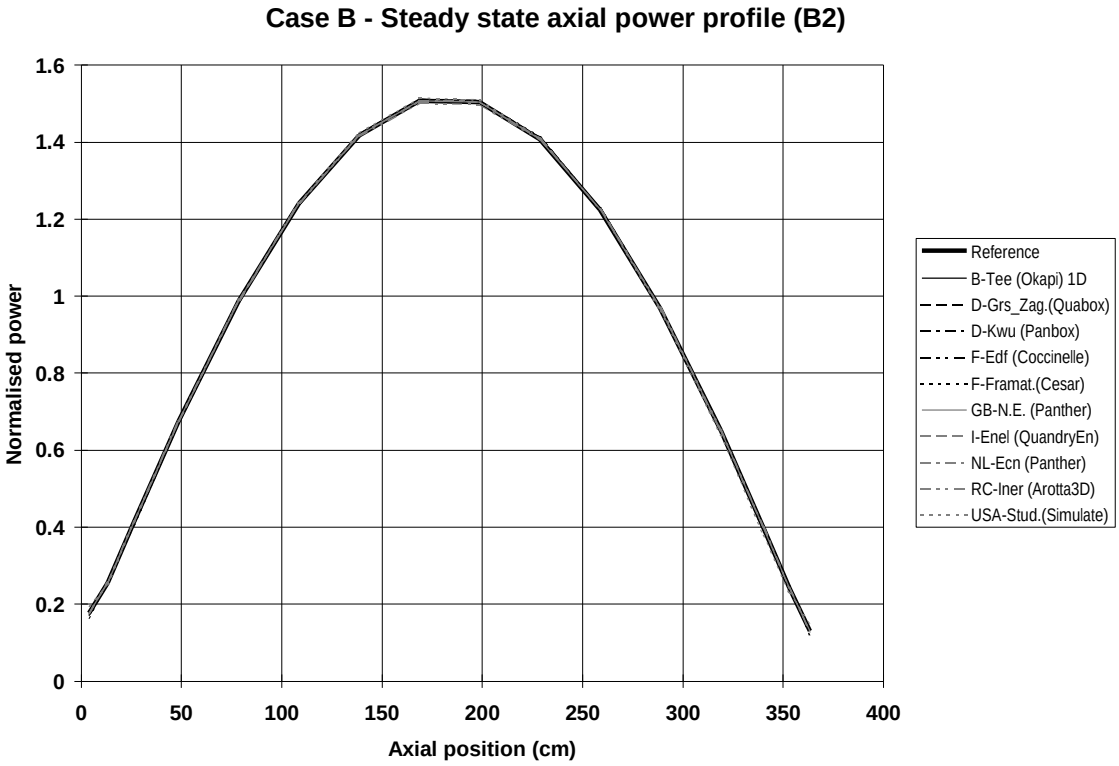
Case B - Steady state axial power profile (B2)
Normalised power
Axial position (cm)
0
0.2
0.4
0.6
0.8
1
1.2
1.4
1.6
0
50
100
150
200
250
300
350
400
Reference
B-Tee (Okapi) 1D
D-Grs_Zag.(Quabox)
D-Kwu (Panbox)
F-Edf (Coccinelle)
F-Framat.(Cesar)
GB-N.E. (Panther)
I-Enel (QuandryEn)
NL-Ecn (Panther)
RC-Iner (Arotta3D)
USA-Stud.(Simulate)

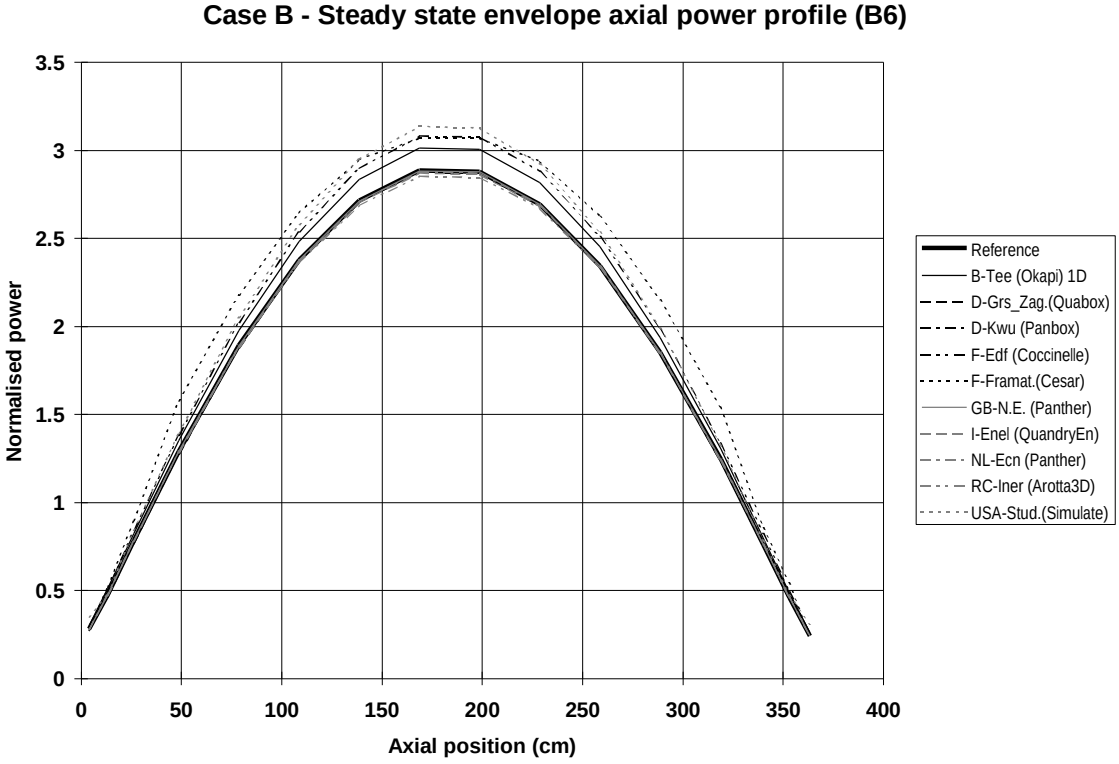
Case B - Steady state envelope axial power profile (B6)
Normalised power
Axial position (cm)
0
0.5
1
1.5
2
2.5
3
3.5
0
50
100
150
200
250
300
350
400
Reference
B-Tee (Okapi) 1D
D-Grs_Zag.(Quabox)
D-Kwu (Panbox)
F-Edf (Coccinelle)
F-Framat.(Cesar)
GB-N.E. (Panther)
I-Enel (QuandryEn)
NL-Ecn (Panther)
RC-Iner (Arotta3D)
USA-Stud.(Simulate)

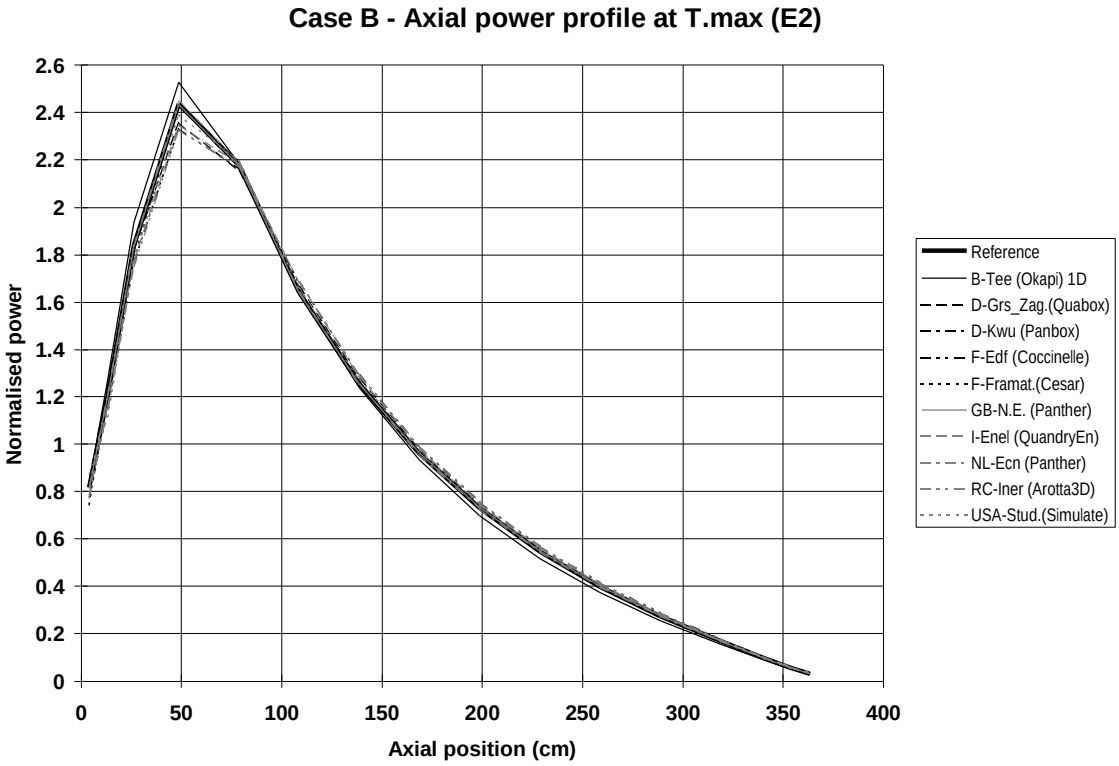
Case B - Axial power profile at T.max (E2)
Normalised power
Axial position (cm)
Reference
B-Tee (Okapi) 1D
D-Grs_Zag.(Quabox)
D-Kwu (Panbox)
F-Edf (Coccinelle)
F-Framat.(Cesar)
GB-N.E. (Panther)
I-Enel (QuandryEn)
NL-Ecn (Panther)
RC-Iner (Arotta3D)
USA-Stud.(Simulate)

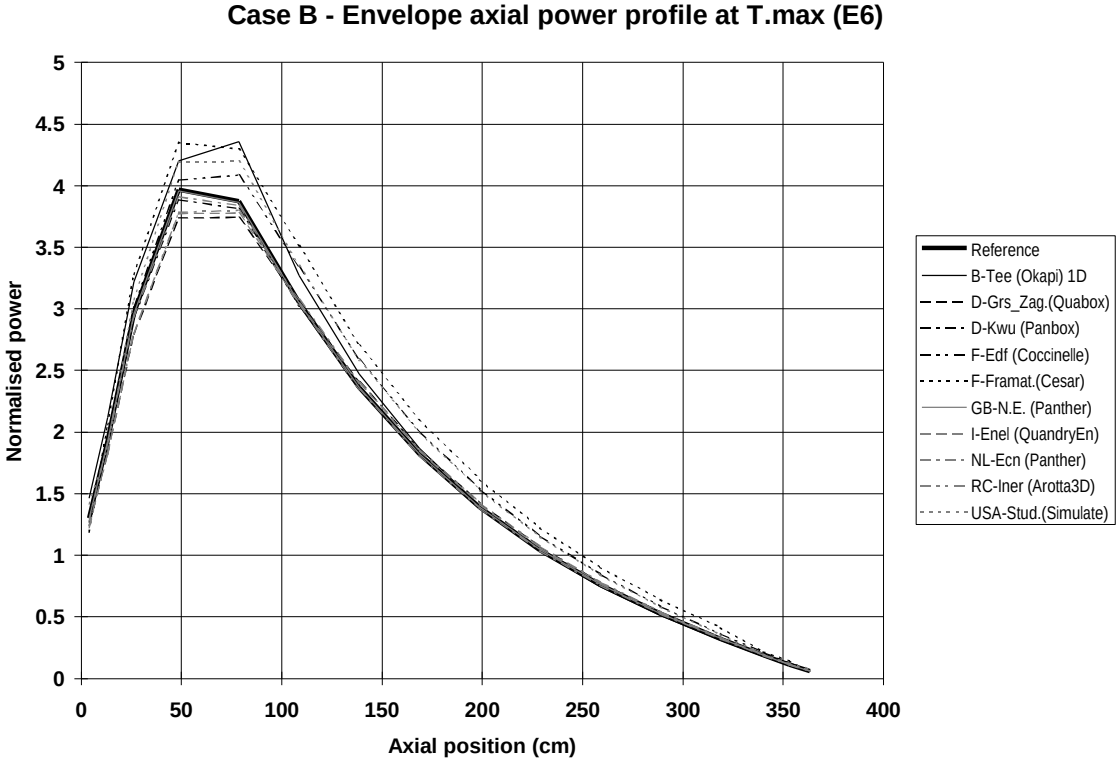
Case B - Envelope axial power profile at T.max (E6)
Normalised power
Axial position (cm)
Reference
B-Tee (Okapi) 1D
D-Grs_Zag.(Quabox)
D-Kwu (Panbox)
F-Edf (Coccinelle)
F-Framat.(Cesar)
GB-N.E. (Panther)
I-Enel (QuandryEn)
NL-Ecn (Panther)
RC-Iner (Arotta3D)
USA-Stud.(Simulate)

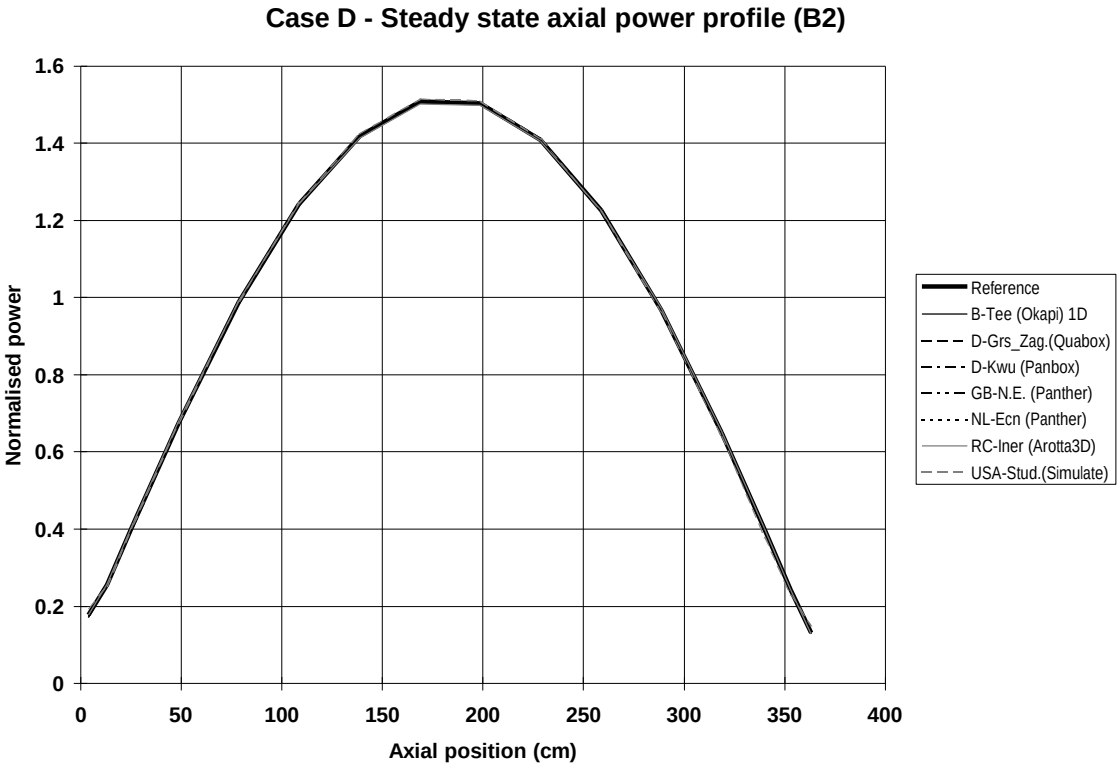
Case D - Steady state axial power profile (B2)
Normalised power
Axial position (cm)
0
0.2
0.4
0.6
0.8
1
1.2
1.4
1.6
0
50
100
150
200
250
300
350
400
Reference
B-Tee (Okapi) 1D
D-Grs_Zag.(Quabox)
D-Kwu (Panbox)
GB-N.E. (Panther)
NL-Ecn (Panther)
RC-Iner (Arotta3D)
USA-Stud.(Simulate)

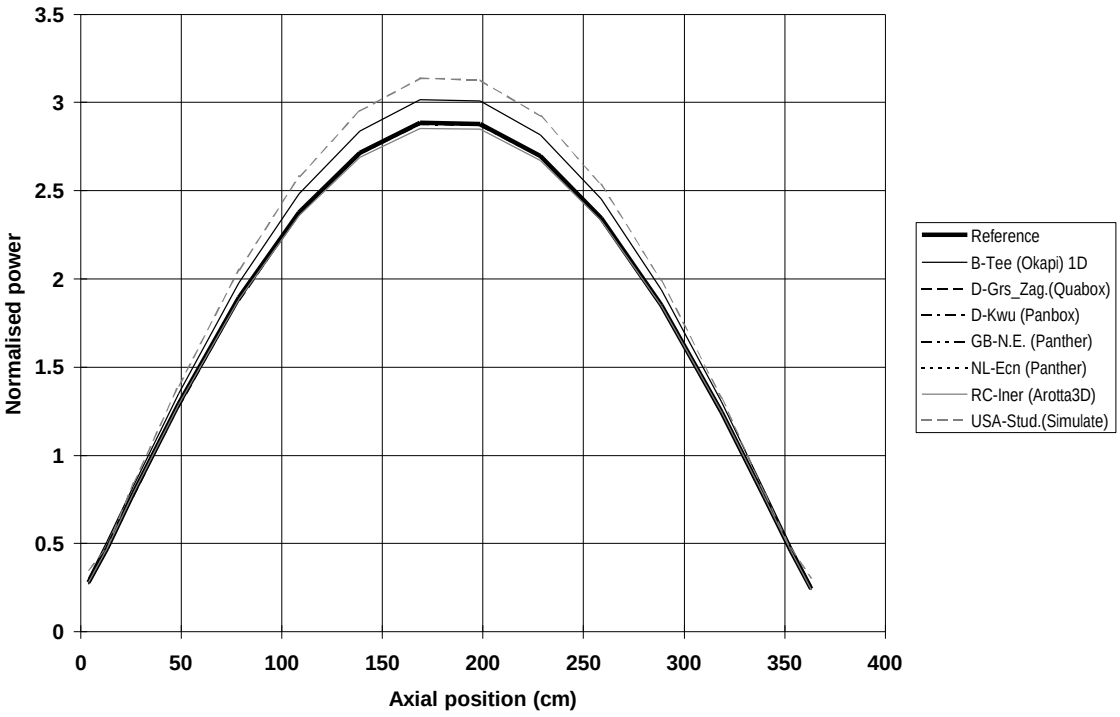
Case D - Steady state envelope axial power profile (B6)
Normalised power
Axial position (cm)
0
0.5
1
1.5
2
2.5
3
3.5
0
50
100
150
200
250
300
350
400
Reference
B-Tee (Okapi) 1D
D-Grs_Zag.(Quabox)
D-Kwu (Panbox)
GB-N.E. (Panther)
NL-Ecn (Panther)
RC-Iner (Arotta3D)
USA-Stud.(Simulate)

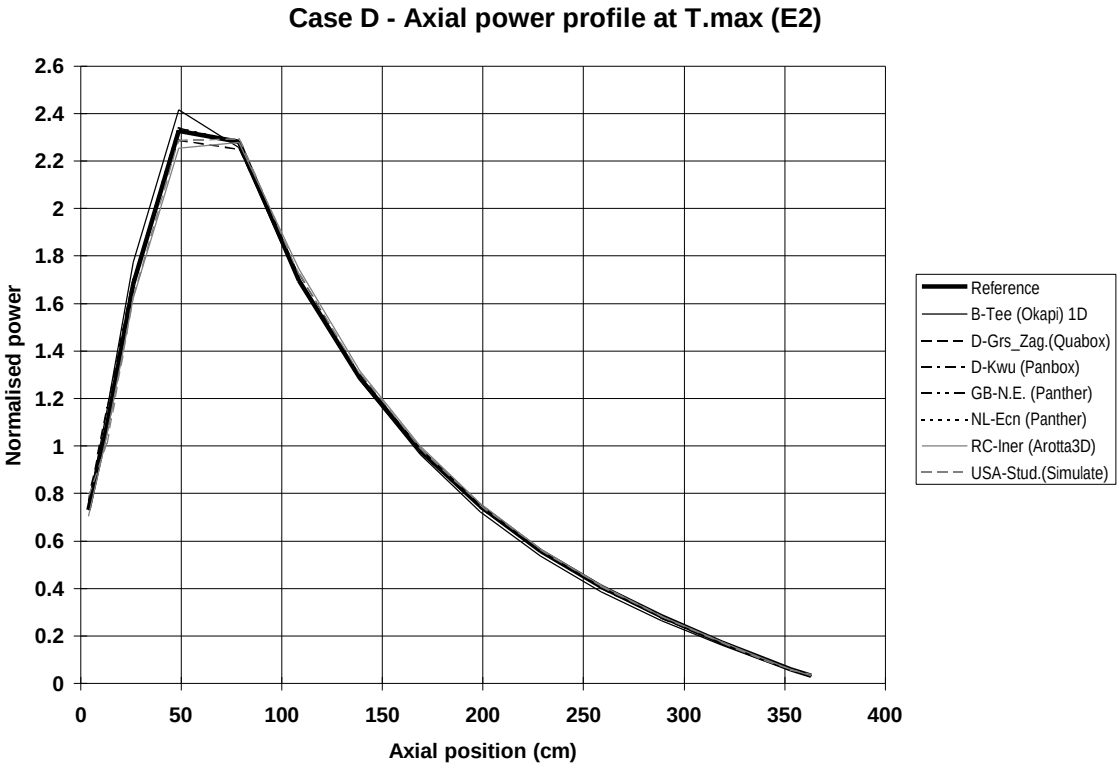
Case D - Axial power profile at T.max (E2)
Normalised power
Axial position (cm)
0
0.2
0.4
0.6
0.8
1
1.2
1.4
1.6
1.8
2
2.2
2.4
2.6
0
50
100
150
200
250
300
350
400
Reference
B-Tee (Okapi) 1D
D-Grs_Zag.(Quabox)
D-Kwu (Panbox)
GB-N.E. (Panther)
NL-Ecn (Panther)
RC-Iner (Arotta3D)
USA-Stud.(Simulate)

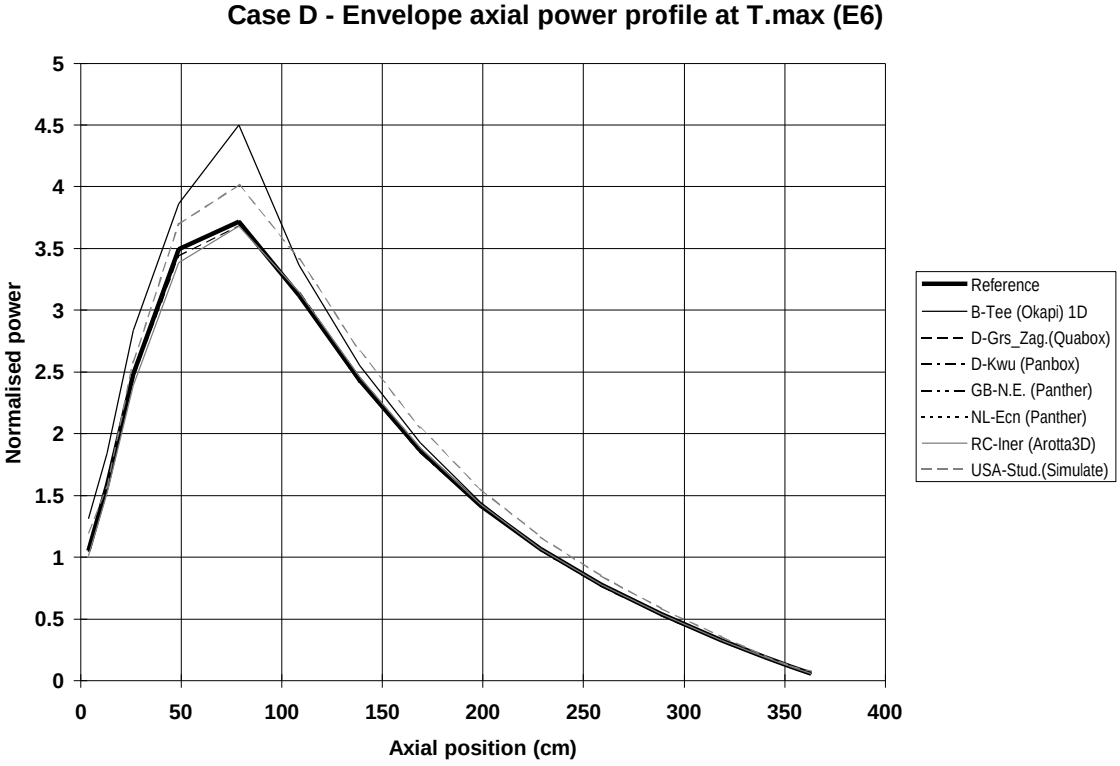
Case D - Envelope axial power profile at T.max (E6)
Normalised power
Axial position (cm)
0
0.5
1
1.5
2
2.5
3
3.5
4
4.5
5
0
50
100
150
200
250
300
350
400
Reference
B-Tee (Okapi) 1D
D-Grs_Zag.(Quabox)
D-Kwu (Panbox)
GB-N.E. (Panther)
NL-Ecn (Panther)
RC-Iner (Arotta3D)
USA-Stud.(Simulate)

APPENDIX D

Radial power profiles

The following plots are given for Cases A, B and D; the results for Case C are very close to those obtained for Case B and have therefore been omitted here:

- steady state average power distribution (B3);
- steady state radial power distribution in axial layer 6 (B4);
- steady state radial power distribution in axial layer 13 (B5);
- average power distribution at time of power maximum (E3);
- radial power distribution in axial layer 6 at time of power maximum (E4);
- radial power distribution in axial layer 13 at time of power maximum (E5).

Axial layers 6 and 13 are located as follows:

- layer 6 is centred at 108.7 cm from bottom of active core, where one expects to find the power peak during rod extraction;
- layer 13 is centred at 318.7 cm from bottom of active core, where one expects a strongly deformed radial profile during the transient, due to the presence of the control rods.

Remark

Plotting together ten different radial power profiles is a difficult matter. The purpose of this plot, however, is only to identify possible discrepancies. We therefore developed the 26 nodes on a straight line. The last eight nodes (19-26) represent a median slice of the core, as shown on figure below.

I	J	K	L	M	N	O	P	
				1	2			**5**
			3	4	5	6		**6**
		7	8	9	10	11		**7**
	12	13	14	15	16	17	18	**8**
19	20	21	22	23	24	25	26	**9**

- The results obtained by INER (Arotta-3D) for axial layers 6 and 13 seem to differ from the average only by a constant factor; we suspect the normalisation as the source of the discrepancy: relative to layer average power instead of core average power.